

Morphoelastic Rods

Part I: A Single Growing Elastic Rod

D.E. Moulton, T. Lessinnes, A. Goriely*

OCCAM, Institute of Mathematics, University of Oxford, Oxford, UK

Abstract

A theory for the dynamics and statics of growing elastic rods is presented. First, a single growing rod is considered and the formalism of three-dimensional multiplicative decomposition of morphoelasticity is used to describe the bulk growth of Kirchhoff elastic rods. Possible constitutive laws for growth are discussed and analysed. Second, a rod constrained or glued to a rigid substrate is considered, with the mismatch between the attachment site and the growing rod inducing stress. This stress can eventually lead to instability, bifurcation, and buckling.

Contents

1	Introduction	2
2	Classic rod theory	3
2.1	Kinematics	3
2.1.1	The case of unshearable rods	5
2.2	The mechanics of Kirchhoff rods	6
2.3	Constitutive laws	6
2.3.1	Extensible and shearable rods	6
2.3.2	Inextensible and unshearable rods	7
2.3.3	Constitutively isotropic extensible and unshearable rods with quadratic energy	7
3	A single morphoelastic rod	8
3.1	Kinematics of a growing rod	8
3.2	Mechanics of a growing rod	9
3.3	Constitutive and evolution laws for a single growing rod	10
3.4	Evolution law for a growing rod	10
4	A growing rod on a foundation	11
5	Buckling criterion	12
5.1	The perturbation expansion	13
5.2	Bifurcation criterion	14
6	Growing rings	14
6.1	Without external force	14
6.1.1	Remodeling	15
6.1.2	Post buckling regime	15
6.1.3	Fourier modes for the buckled ring	16
6.2	Growing ring on a foundation	17
6.2.1	Foundation inside	18
6.2.2	Foundation underneath	19

*Corresponding author; email: goriely@maths.ox.ac.uk

7	Growing naturally straight rods	21
7.1	Uniaxial deformation	21
7.2	Planar deformations	23
7.3	Spatial deformations	25
8	Conclusions	28
A	How body couples are generated	35
B	Computation of the Fourier coefficients for the growing ring	35

1. Introduction

Filamentary structures can be observed in nature at all scales, from the microscopic chains of molecules to the macroscopic braided magnetic flux tubes in solar flares. Due to their geometric similarity and despite their widely different length scales and microscopic structures, filaments of all sizes seem to grow, move, and change shape according to universal laws. For instance, when a straight rope is twisted sufficiently, it will begin to coil on itself. The same change of configuration is observed to occur in bacterial fibers, DNA molecules and telephone cables [1]. Understanding the growth, formation and dynamics of these fundamental structures is not only of intrinsic theoretical interest, but it also lies at the heart of a host of important processes in biology, physics, and engineering [2, 3, 4, 5, 6, 7, 8, 9, 10].

The main motivation for the research presented here is the fascinating growth of various biofilaments as observed in bacterial fibers [11, 12, 1, 13], bacterial filaments [14, 15, 16, 17], fungi [18, 19, 20, 21], root hairs [22, 23, 24], stems [25, 26, 27, 28, 29, 30], roots [31, 32, 33, 34, 35], tendrils [36, 37, 38, 39], neurons [40, 41, 42, 43, 44, 45], umbilical cords [46, 47], tendons [48], arteries [49, 50, 51], and the spine [52], to name but a few.

On the mechanical side, there is a considerable body of work and current interest in volumetric three-dimensional growth theories, dating back to Skalak and Hoger's seminal work [53, 54, 55] as well as [56, 57]. The ensuing equations are however difficult to study both analytically and numerically. Furthermore, a general constitutive theory relating growth to stresses is still lacking [58]. Due to its relative geometric simplicity, a one-dimensional theory of growing rods is best suited for deriving growth laws from basic principles. *A priori* genetic, biochemical, and micro-structural information must be combined in order to obtain an effective macroscopic theory of growth, but the first step is to develop a general mathematical framework for growing slender structures.

Filamentary growth is seen to occur in different ways. The first notable aspect of growth is extensional, an overall increase in the length of the filament. Many biological filaments constrained by their surrounding medium are known to extend in a small zone close to the free end, a process known as *tip growth* [59] and first reported for root hairs by Duhamel du Monceau in 1758 [60]. However, when biofilaments do not have to penetrate through a dense medium, they are often seen to have distributed growth along their length [11, 15, 61]. Together with a primary extensional growth, a secondary growth is also observed. In this process, typical for plants [62, 63, 64], the structure also increases in thickness and density. If primary or secondary growth does not occur uniformly in the section, differential growth develops and the structure develops residual stresses, known as tissue-tension in plants [65, 66, 67]. If these stresses are sufficiently important, the structure may buckle or develop curvature. In a two-dimensional setting, the simplest case of growth-induced buckling is the classical theory of thermal buckling of a bimetallic beam first developed by Timoshenko [68]. In that process, two straight metallic beams with different thermal expansion coefficients are fastened together. Under a change of temperature, one beam expands faster than the other and induces buckling on the entire structure [69, 70]. In growing plants, differential growth is also the main mechanism for gravitropic response [71, 72, 73]. In a three-dimensional setting, it is known that curvature is closely coupled to both torsion and twist. Therefore, induced curvature can also result in torsion and twist. For instance, the dorsal side of tendrils is known to grow faster than its ventral side, inducing curvature, an observation first reported by de Vries in 1880. When tendrils are attached and are in tension, they are not free to roll-up on themselves and naturally develop torsion and twist by forming helical structures with opposite handedness, a phenomenon known as tendril perversion [38]. Torsion and twist can also be directly induced when differential growth does not occur symmetrically, a much more subtle problem that leads

directly to torsion. This is often referred to as *helical growth* and is observed in bacteria [11], fungi [21], and plants [74, 28, 26, 75].

We include in our discussion of growth aspects of both growth (increase in body mass) and remodeling (change of material properties). In a reduced theory, these two distinct phenomena are mixed as typically growth and remodeling both change the intrinsic material properties of the rod.

At the mathematical level, the growth of biological filaments involves interesting aspects of curve dynamics [76, 77]. A natural starting point for the modeling of biofilaments is to consider them as thin elastic rods subjected to external constraints. The basic idea is to cross-sectionally average all the stresses along the space curve representing the centreline of the rod. This procedure leads to the Kirchhoff equations [78, 79, 80, 81, 1], relating averaged forces and moments to the curve's strains (characterized by the curvatures, shears, and extension). These equations provide the starting point for much theoretical analysis and numerical modeling. Various aspects of a theory of growing elastic Kirchhoff rods were first discussed in [39, 28, 13, 37, 1] mostly in biological contexts, and, more recently O'Reilly and co-workers developed a theory of planar growing plants with special emphasis on tip growth, branching, and constitutive laws [82, 83, 84] (see also [85] for a 3D extension). Other related works include elastic growth in a fluid environment [86, 87] and thermo-elastic rods [88, 89, 90].

The theory of growing three-dimensional structures requires great care as growth, through incompatibility, naturally changes the geometry of the reference configuration. To capture this effect, a multiplicative decomposition of the deformation gradient can be used as first proposed in [55], or equivalently by modifying the geometric properties of the reference configuration [91]. Incompatible growth induces local, pointwise residual stresses in the material, independently of the global arrangement of the elastic object or boundary conditions. However, in a one-dimensional structure allowed to grow axially and in girth, no such residual stress can be created since the equivalent of the deformation gradient (played by the stretches) is always compatible. This lack of incompatibility greatly simplifies the theory as the local effect of growth can easily be captured by a re-parameterization of the arc length and a change of the material property. Nevertheless, a growing structure can develop stresses due either to its global geometry (a closed ring growing in length will develop bending moments), or boundary conditions (a straight growing rod between two plates, a rod attached to a foundation, or two rods attached to each other growing at different rates). In turn, these stresses can be sufficient to cause a buckling instability, a primary focus of the present work.

The paper is organised as follows. First, for the sake of setting the general framework, we tersely summarise the classical theory of Kirchhoff elastic rods by recalling the geometry and balance laws for mechanical quantities attached to a space curve representing the filament in space. Second, we consider the problem of a single growing rod. Then, we demonstrate the developed growth framework through a series of examples. In particular, we investigate possible growth related buckling instabilities in rods attached to a rigid foundation.

2. Classic rod theory

2.1. Kinematics

We define a dynamical *space curve* $\mathbf{r}(S, T)$ as a smooth function of a material parameter S and time T , i.e. $\mathbf{r} : \mathbb{R}^2 \rightarrow \mathbb{R}^3$. At any time T the arc length s is defined as

$$s = \int_0^S \left| \frac{\partial \mathbf{r}(\sigma, T)}{\partial \sigma} \right| d\sigma. \quad (1)$$

The unit tangent vector $\boldsymbol{\tau}$ to the space curve, \mathbf{r} , is

$$\boldsymbol{\tau} = \frac{\partial \mathbf{r}}{\partial s}, \quad (2)$$

and we can construct the standard *Frenet-Serret frame* of tangent $\boldsymbol{\tau}$, normal $\boldsymbol{\nu}$, and binormal $\boldsymbol{\beta}$, vectors which form a right-handed orthonormal basis on \mathbf{r} . Along the curve, this triad moves as a function of arc

length according to the *Frenet-Serret equations*:

$$\frac{\partial \boldsymbol{\tau}}{\partial s} = \kappa \boldsymbol{\nu}, \quad (3)$$

$$\frac{\partial \boldsymbol{\nu}}{\partial s} = \tau \boldsymbol{\beta} - \kappa \boldsymbol{\tau}, \quad (4)$$

$$\frac{\partial \boldsymbol{\beta}}{\partial s} = -\tau \boldsymbol{\nu}, \quad (5)$$

where the *curvature*

$$\kappa = \left| \frac{\partial \boldsymbol{\tau}}{\partial s} \right| \quad (6)$$

measures the turning rate of the tangent along the curve and is given by the inverse of the radius of the best fitting circle at a given point. The *torsion* τ measures the rotation of the Frenet triad around the tangent $\boldsymbol{\tau}$ as a function of arc length and is related to the non-planarity of the curve. If the curvature and torsion are known for all s , the frame $(\boldsymbol{\nu}, \boldsymbol{\beta}, \boldsymbol{\tau})$ can be obtained as the unique solution of the Frenet-Serret equations up to a translation and rotation of the curve. The space curve \mathbf{r} is obtained by integrating the tangent vector $\boldsymbol{\tau}$, using (2).

In order to study the motion of elastic filamentary structures, we need to generalize the notion of space curves to rods. Geometrically, a *rod* is defined by its centerline $\mathbf{r}(S, T)$ where T is time and S is a material parameter taken to be the arc length in a stress free configuration ($0 \leq S \leq L$) and two orthonormal vector fields $\mathbf{d}_1(S, T)$, $\mathbf{d}_2(S, T)$ representing the orientation of a material cross section at S [78, 92, 93]. We define the *stretch* by $\alpha = \frac{\partial s}{\partial S}$, where s is the current arc length as above. A local orthonormal basis is obtained (see Figure 1) by defining $\mathbf{d}_3(S, T) = \mathbf{d}_1(S, T) \times \mathbf{d}_2(S, T)$ and a complete kinematic description is given by:

$$\frac{\partial \mathbf{r}}{\partial S} = \mathbf{v}, \quad (7)$$

$$\frac{\partial \mathbf{d}_i}{\partial S} = \mathbf{u} \times \mathbf{d}_i, \quad i = 1, 2, 3, \quad (8)$$

$$\frac{\partial \mathbf{d}_i}{\partial T} = \mathbf{w} \times \mathbf{d}_i \quad i = 1, 2, 3, \quad (9)$$

where \mathbf{u} , \mathbf{v} are the *strain* vectors and \mathbf{w} is the *spin* vector. Note that the orthonormal frame $(\mathbf{d}_1, \mathbf{d}_2, \mathbf{d}_3)$ is different, in general from the Frenet-Serret frame.

The components of a vector $\mathbf{a} = a_1 \mathbf{d}_1 + a_2 \mathbf{d}_2 + a_3 \mathbf{d}_3$ in the local basis are denoted by $\mathbf{a} = (a_1, a_2, a_3)$.¹ The first two components v_1, v_2 of the *stretch vector* \mathbf{v} represent transverse shearing of the cross-sections while $v_3 > 0$ is associated with stretching and compression. Since the vectors \mathbf{d}_i are normalized, the norm of \mathbf{v} gives the stretch of the rod during deformation: $\alpha = |\mathbf{v}| = |\mathbf{v}|$. The first two components u_1, u_2 of the *Darboux vector* \mathbf{u} are associated with bending while u_3 represents twisting, that is the rotation of the basis (not the curve) around the \mathbf{d}_3 vector. To understand the mathematical structure of the system, it is convenient to introduce a matrix describing the basis

$$\mathbf{D} = \begin{pmatrix} \mathbf{d}_1 & \mathbf{d}_2 & \mathbf{d}_3 \end{pmatrix}, \quad (10)$$

so that $\mathbf{a} = \mathbf{D}\mathbf{a}$. Then, an alternative representation of the kinematics is obtained in terms of matrices by introducing, respectively, the *twist matrix* $\mathbf{U}(s, t)$ and the *spin matrix* $\mathbf{W}(s, t)$ as follows

$$\frac{\partial \mathbf{D}}{\partial S} \equiv \begin{pmatrix} \frac{\partial \mathbf{d}_1}{\partial S} & \frac{\partial \mathbf{d}_2}{\partial S} & \frac{\partial \mathbf{d}_3}{\partial S} \end{pmatrix} = \mathbf{D} \cdot \mathbf{U}, \quad (11)$$

$$\frac{\partial \mathbf{D}}{\partial T} \equiv \begin{pmatrix} \frac{\partial \mathbf{d}_1}{\partial T} & \frac{\partial \mathbf{d}_2}{\partial T} & \frac{\partial \mathbf{d}_3}{\partial T} \end{pmatrix} = \mathbf{D} \cdot \mathbf{W}. \quad (12)$$

These matrices are the skew-symmetric matrices associated with the axial vectors \mathbf{u} and \mathbf{w} respectively,

$$\mathbf{U} = \begin{pmatrix} 0 & -u_3 & u_2 \\ u_3 & 0 & -u_1 \\ -u_2 & u_1 & 0 \end{pmatrix}, \quad \mathbf{W} = \begin{pmatrix} 0 & -w_3 & w_2 \\ w_3 & 0 & -w_1 \\ -w_2 & w_1 & 0 \end{pmatrix}. \quad (13)$$

¹Following [92], we use the *sans-serif* fonts to denote the components of a vector in the local basis.

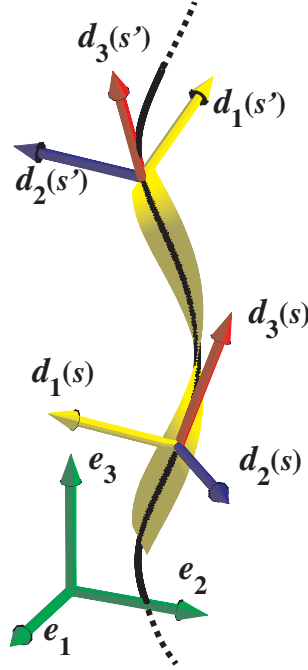


Figure 1: The director basis represents the orientation of the material cross section along the rod.

The entries of \mathbf{U} and \mathbf{W} are not independent. By differentiating (11) with respect to time and (12) with respect to arc length and then equating their cross-derivatives, we obtain a compatibility relation for \mathbf{U} and \mathbf{W} :

$$\frac{\partial \mathbf{U}}{\partial T} - \frac{\partial \mathbf{W}}{\partial S} = [\mathbf{U}, \mathbf{W}], \quad (14)$$

where $[\mathbf{U}, \mathbf{W}] = \mathbf{U}\mathbf{W} - \mathbf{W}\mathbf{U}$. The two linear systems (11) and (12) can be seen as a Lax pair for the nonlinear partial differential equations generated by the compatibility condition (14). Indeed, the natural kinematic structure of evolving rods has led to a large and beautiful body of work connecting the motion of curves with integrable systems [94, 95, 96, 97, 98]. However, this construction is purely geometric and has little to do with evolution of elastic rods as governed by mechanical principles.

2.1.1. The case of unshearable rods

A particularly important class of rods is obtained by taking $\mathbf{v}_1 = \mathbf{v}_2 = 0$, $\mathbf{v}_3 = \alpha$. In this case the possible deformations are restricted so that the vectors spanning the cross sections remain perpendicular to the axis. Geometrically, the vectors $(\mathbf{d}_1, \mathbf{d}_2)$ lie in the normal plane to the axis and are related to the normal and binormal vectors by a rotation through the *register angle* φ ,

$$\mathbf{d}_1 = \boldsymbol{\nu} \cos \varphi + \boldsymbol{\beta} \sin \varphi, \quad (15)$$

$$\mathbf{d}_2 = -\boldsymbol{\nu} \sin \varphi + \boldsymbol{\beta} \cos \varphi, \quad (16)$$

$$\mathbf{d}_3 = \boldsymbol{\tau} \quad (17)$$

This rotation implies that

$$\mathbf{u} = \alpha(\kappa \sin \varphi, \kappa \cos \varphi, \tau + \frac{1}{\alpha} \frac{\partial \varphi}{\partial S}) \quad (18)$$

where κ and τ are the usual *Frenet curvature and torsion*. These relations can also be inverted to yield φ , κ and τ as functions of the twist vector components:

$$\cot \varphi = \frac{u_2}{u_1}, \quad (19)$$

$$\kappa = \frac{1}{\alpha} \sqrt{u_1^2 + u_2^2}, \quad (20)$$

$$\tau = \frac{1}{\alpha} \left(u_3 + \frac{u_2' u_1 - u_1' u_2}{u_1^2 + u_2^2} \right). \quad (21)$$

The quantities τ , $\frac{\partial \varphi}{\partial S}$ and u_3 play related but distinct roles. The torsion τ is a property of the curve alone and is a measure of its non-planarity. Hence a curve with null torsion is a plane curve, and any two rods having the same curvature and torsion for all S and T have the same space curve \mathbf{r} as axis, and can only be distinguished by the orientation of the local basis. The quantity $\frac{\partial \varphi}{\partial S}$, the *excess twist*, is a property of the rod alone, representing the rotation of the local basis with respect to the Frenet frame as the arc length increases. An untwisted rod, characterized by $\frac{\partial \varphi}{\partial S} = 0$ is therefore called a *Frenet rod*. In a Frenet rod, the angle φ between the binormal \mathbf{b} and the vector field \mathbf{d}_2 is constant, hence the binormal is representative of the orientation of the local basis $(\mathbf{d}_1, \mathbf{d}_2, \mathbf{d}_3)$. The twist density, u_3 , is a property of both the space curve and the rod, measuring the total rotation (as can be seen from the third component of (18)) of the local basis around the space curve as the arc length increases.

2.2. The mechanics of Kirchhoff rods

Before considering the case of a growing rod, we review the fundamental equations for the dynamics of Kirchhoff rods. The stress acting on the cross section at $\mathbf{r}(S)$ from the part of the rod with $S' > S$ gives rise to a resultant force $\mathbf{n}(S, T)$ and resultant moment $\mathbf{m}(S, T)$ attached to the central curve. The balance of linear and angular momenta yields [92]

$$\frac{\partial \mathbf{n}}{\partial S} + \mathbf{f} = \rho A \frac{\partial^2 \mathbf{r}}{\partial T^2}, \quad (22)$$

$$\frac{\partial \mathbf{m}}{\partial S} + \frac{\partial \mathbf{r}}{\partial S} \times \mathbf{n} + \mathbf{l} = \rho \left(I_2 \mathbf{d}_1 \times \frac{\partial^2 \mathbf{d}_1}{\partial T^2} + I_1 \mathbf{d}_2 \times \frac{\partial^2 \mathbf{d}_2}{\partial T^2} \right), \quad (23)$$

where $\mathbf{f}(S, T)$ and $\mathbf{l}(S, T)$ are the body force and couple per unit stress-free length applied on the cross section at S . These body forces and couple can be used to model different effects such as short and long range interactions between different parts of the rod or can be the result of active stress, self-contact, or contact with another body. $A(S)$ is the cross-sectional area (in the stress-free frame), $\rho(S)$ the mass density (mass per unit stress-free volume), and $I_{1,2}(S)$ are the second moments of area of the cross section corresponding to the directions $\mathbf{d}_{1,2}$ at a material point S . Explicitly, they read

$$I_1 = \int_S x_2^2 dx_1 dx_2, \quad I_2 = \int_S x_1^2 dx_1 dx_2. \quad (24)$$

where S is the section at point S and a point on this section is given by a pair $\{x_1, x_2\}$ and located at $\mathbf{r}(S) + x_1 \mathbf{d}_1(S) + x_2 \mathbf{d}_2(S)$ (see Figure 2).

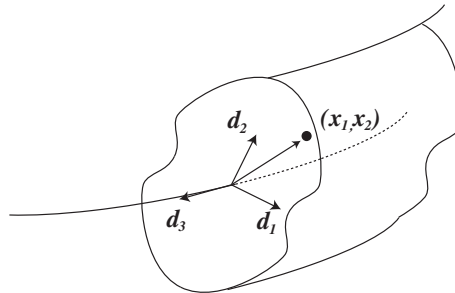


Figure 2: Cross-section of a rod and local coordinates

To close the system, we assume that the resultant stresses are related to the strains. Again, there are two important cases to distinguish.

2.3. Constitutive laws

2.3.1. Extensible and shearable rods

First, we consider the case where the rod is extensible and shearable and we assume that the rod is hyperelastic. That is, we assume that there exists a strain-energy density function $W = W(\mathbf{y}, \mathbf{z}, s)$ such that the constitutive relations for the resultant moment and force in the local basis are given by

$$\mathbf{m} = \mathbf{f}(\mathbf{u} - \hat{\mathbf{u}}, \mathbf{v} - \hat{\mathbf{v}}, S) = \partial_{\mathbf{y}} W(\mathbf{u} - \hat{\mathbf{u}}, \mathbf{v} - \hat{\mathbf{v}}, S), \quad (25)$$

$$\mathbf{n} = \mathbf{g}(\mathbf{u} - \hat{\mathbf{u}}, \mathbf{v} - \hat{\mathbf{v}}, S) = \partial_{\mathbf{z}} W(\mathbf{u} - \hat{\mathbf{u}}, \mathbf{v} - \hat{\mathbf{v}}, S), \quad (26)$$

where $\hat{\mathbf{v}}, \hat{\mathbf{u}}$ are the strains in the unstressed configuration ($\mathbf{m} = \mathbf{n} = \mathbf{0}$ when $\mathbf{u} = \hat{\mathbf{u}}, \mathbf{v} = \hat{\mathbf{v}}$). Without loss of generality, one can choose the general basis so that $\hat{v}_1 = \hat{v}_2 = 0$. Furthermore, if S is the arc length of the unstressed configuration then $\hat{v}_3 = 1$. Typically, W is assumed to be continuously differentiable, convex, and coercive. The rod is *uniform* if its material properties do not change along its length (*i.e.* W has no explicit dependence on s) and the stress-free strains $\hat{\mathbf{v}}, \hat{\mathbf{u}}$ are independent of s .

2.3.2. Inextensible and unshearable rods

In the second case, we assume that the rod is inextensible and unshearable, that is we take $\mathbf{v} = \mathbf{d}_3$ and the material parameter $S = s$ becomes the arc length. In that case, there is no constitutive relationship for the resultant force and the strain-energy density is a function only of $(\mathbf{u} - \hat{\mathbf{u}})$, that is

$$\mathbf{m} = \partial_{\mathbf{y}} W(\mathbf{u} - \hat{\mathbf{u}}) = \mathbf{f}(\mathbf{u} - \hat{\mathbf{u}}). \quad (27)$$

For a quadratic strain energy $W = \mathbf{y}^T \mathbf{K} \mathbf{y}$, the constitutive relations for the local basis components \mathbf{m} are

$$\mathbf{m} = \mathbf{K}(\mathbf{u} - \hat{\mathbf{u}}), \quad \mathbf{K} = \begin{pmatrix} K_1 & K_{12} & K_{13} \\ K_{12} & K_2 & K_{23} \\ K_{13} & K_{23} & K_3 \end{pmatrix}, \quad K_1 \leq K_2. \quad (28)$$

Note that, in general, due to the arbitrary phase in the definition of the general basis, one can choose the vector \mathbf{d}_1 so that either $K_{12} = K_{21} \equiv 0$ or $\hat{u}_1 \equiv 0$ or $\hat{u}_2 \equiv 0$. In the simplest, and most widely used, case the energy is further simplified to

$$W_1 = K_1(u_1 - \hat{u}_1)^2 + K_2(u_2 - \hat{u}_2)^2 + K_3(u_3 - \hat{u}_3)^2, \quad (29)$$

where $\hat{\mathbf{u}}$ is the unstressed Darboux vector that defines the shape of the rod when unloaded. Explicitly, the resultant moment and coefficients $\{K_1, K_2, K_3\}$ are

$$\mathbf{m} = EI_1(u_1 - \hat{u}_1)\mathbf{d}_1 + EI_2(u_2 - \hat{u}_2)\mathbf{d}_2 + \mu J(u_3 - \hat{u}_3)\mathbf{d}_3 \quad (30)$$

where E is the Young's modulus, μ is the shear modulus, J is a parameter that depends on the cross-section shape and I_1 and I_2 are the second moments of area given by (24) (an explicit form for J and examples can be found in [99]).

For the simple but important case of a rod with uniform circular cross section of radius R , these parameters are:

$$I_1 = I_2 = \frac{J}{2} = \frac{\pi R^4}{4}. \quad (31)$$

The products $EI_1 \equiv K_1$ and $EI_2 \equiv K_2$ are the *principal bending stiffnesses* of the rod, and $\mu J \equiv K_3$ is the *torsional stiffness*. Upon rescaling (see [99]), the properties of the rod can be conveniently described by a single parameter, the ratio of bending to torsional stiffness,

$$\Gamma \equiv \frac{\mu J}{EI_1} = \frac{1}{1 + \sigma} \in \left[\frac{2}{3}, 1 \right]. \quad (32)$$

where σ denotes the Poisson ratio.

2.3.3. Constitutively isotropic extensible and unshearable rods with quadratic energy

For many applications, rods can be modeled as inextensible and unshearable. However, for the modeling of a growing rod, it is also interesting to consider the case where the rod is unshearable but extensible with a quadratic energy that is constitutively isotropic. In this case, in addition to (29), we have an equation relating the elastic stretch $\alpha \equiv v_3 \equiv \frac{\partial s}{\partial S}$ to the tension

$$\mathbf{m} = EI_1(u_1 - \hat{u}_1)\mathbf{d}_1 + EI_2(u_2 - \hat{u}_2)\mathbf{d}_2 + \mu J(u_3 - \hat{u}_3)\mathbf{d}_3, \quad (33)$$

$$n_3 = EA(\alpha - 1). \quad (34)$$

For a straight rod under uniaxial tension, this last constitutive equation is simply Hooke's law. Note that although the Darboux vector \mathbf{u} is scaled by a factor α in (18), the unstressed Darboux vector $\hat{\mathbf{u}}$ is given by the unstressed geometric curvatures in the reference configuration (it is not scaled by α since it is a material property of the rod in the reference configuration).

3. A single morphoelastic rod

From a modeling perspective, we can take advantage of the fact that growth in filamentary structures takes place on time scales much longer than any elastic time scale propagation or viscous relaxation. Indeed, typical elastic time scales are related to elastic wave propagation (with typical velocities of 100 m/s, the associated elastic time scale for a 10 cm long filament is 10^{-3} s), whereas growth time scales are of the order of minutes, hours, and days. Different attempts have been made to model growing rods. Essentially, one can distinguish three different approaches.

The first approach, which we refer to as *parameter variation*, consists in considering families of rod solutions (typically static due to the slow time evolution of growth with respect to viscous damping in the rod) parametrized by one of the material parameters. For instance, in the growth of a tree, one may consider the length and width as two parameters that evolve in time. At each time, we increase the value of such parameters and recompute the static solution that matches the boundary conditions [28].

The second approach is *remodeling*. The idea is now to consider a separate evolution law for the material parameters that may depend on time and history of the material. For instance, an initially straight rod can develop intrinsic curvature and the resulting equilibrium configurations for given boundary conditions can be studied [38, 39]. This is fundamentally different from the previous approach since the material parameters may now be a function of the position and their values depend on the evolution in time.

The third approach presented here, that combines all aspects of growth and remodeling in rods, is to consider the *evolution of the natural configuration*. From the description of the general theory of rods, we see that rods are characterised by intensive quantities such as density and cross-sectional area, and one extensive quantity, the length. It is useful in the theory of morphoelasticity to distinguish between growth and remodeling. Growth refers to a change of volume of the unstressed elastic material, whereas remodeling refers to a change of material properties. While this distinction is clear in the general three-dimensional theory of growing elastic bodies, in the theory of rods growth and remodeling are combined. This is due to the fact that rod theory is a reduction from a three-dimensional elastic body to a one-dimensional structure. For instance, the bending stiffness ($K_1 = EI_1$ in Eq. (29)) is a product of a material coefficient, the Young's modulus, and a geometric property, the second moment of area. As the rod grows and remodels, the material can become stiffer and/or increase in radius, both changing the stiffness. Apart from the change in radius, the rod can grow in length. Again, the effect of this type of growth is not obvious as a change of length in a rod can easily be rescaled without affecting the basic equations for the rod deformation. Therefore, the effect of a change of length in a rod can only be appreciated through boundary effects, that is when the rod interacts with its environment, either through boundary conditions on each end of the rod or through a body force or couple connecting the rod with its surrounding. The case where a rod is closed on itself through periodic boundary conditions generates a self-interaction that can lead to stressed configurations, even in the absence of external forces or couples.

In order to describe interesting aspects of growing rods in space, we first define the mechanics of a single growing rod through the evolution of its reference configuration. Second, we consider the case of a growing rod attached to a given rigid curve in space via an elastic force. For instance, one may consider the case of a growing rod attached to a substrate or the case of a growing rod inside a sphere or lying on a cylinder. In a companion paper, we consider growing birods, that is, two rods attached together and growing at different rates ([100]).

For the rest of this paper, our basic assumptions are:

1. The growth dynamics is slow enough so that the unstressed rod is in elastic equilibrium at all time. We use the variable t to denote the slow time evolution. Note that dynamical problems could still be considered at any given slow time. This assumption merely states that the growth dynamics is decoupled from the elastic dynamic of the rod. Nevertheless, in this paper, we will focus only on static problems. That is, we will assume the existence of a dissipative process that takes the rod back to a stable equilibrium much faster than any growth time scale (in particular to assess the dynamic stability).
2. Unless stated otherwise, the rod is assumed to be at all times hyperelastic, unshearable, and characterised by a quadratic strain-energy function W . Due to remodeling and growth, the parameters defining the unstressed shape $\hat{\mathbf{u}}$ and the coefficients of W may be functions of the growth time t .

3.1. Kinematics of a growing rod

Based on the general approach of growth in nonlinear elasticity through a multiplicative decomposition [55, 101], we consider three different configurations for the rod. The *initial configuration* \mathcal{B}_0 is the unstressed

configuration of the rod at time $t = 0$, all quantities in this state are denoted by a subscript 0. The *reference configuration* \mathcal{V} is the unstressed configuration at a given time t and the *current configuration* \mathcal{B} of the rod is the actual configuration of the rod at time t for given external loads, body loads and boundary conditions. Note that at time t the unstressed configuration may not be realizable in the Euclidian space. For instance, starting initially with a ring of radius one and unstressed curvature one and increasing the rod length while keeping the unstressed curvature constant would lead to a stress-free configuration that would be self-penetrating. However, unlike the three-dimensional case, there is no problem with local compatibility and generation of residual stress associated with the local definition of a growth and elastic tensor [102]. Therefore, all local quantities are well-defined and the reference configuration is appropriate for the computation of the current configuration.

At time $t = 0$, the rod is described by its unstressed shape $\hat{\mathbf{u}}_0 = \hat{\mathbf{u}}(S_0, t = 0)$ with arc length S_0 , total length L_0 , density $\rho_0(S_0)$, cross-sectional surface area $A_0(S_0)$ and a stiffness matrix \mathbf{K}_0 . This unstressed shape evolves so that at any given time t the rod has unstressed shape $\hat{\mathbf{u}} = \hat{\mathbf{u}}(S_0, t)$, with arc length S , total length $L(t)$, density $\rho(S_0, t)$, cross-sectional surface area $A(S_0, t)$ and a stiffness matrix \mathbf{K} . In this description, S_0 is now a material parameter. It is related to arc length S of the virtual configuration \mathcal{V} by the *growth stretch* γ , i.e.

$$\gamma(S_0, t) = \frac{\partial S}{\partial S_0}, \quad (35)$$

so that γ characterizes the local increase of length of a material segment located at a material point S_0 at time t . This virtual configuration is required in order to compute the current shape of the rod for given loads and boundary conditions (See Figure3). In the current configuration, the rod has arclength s and total length $l(t)$.

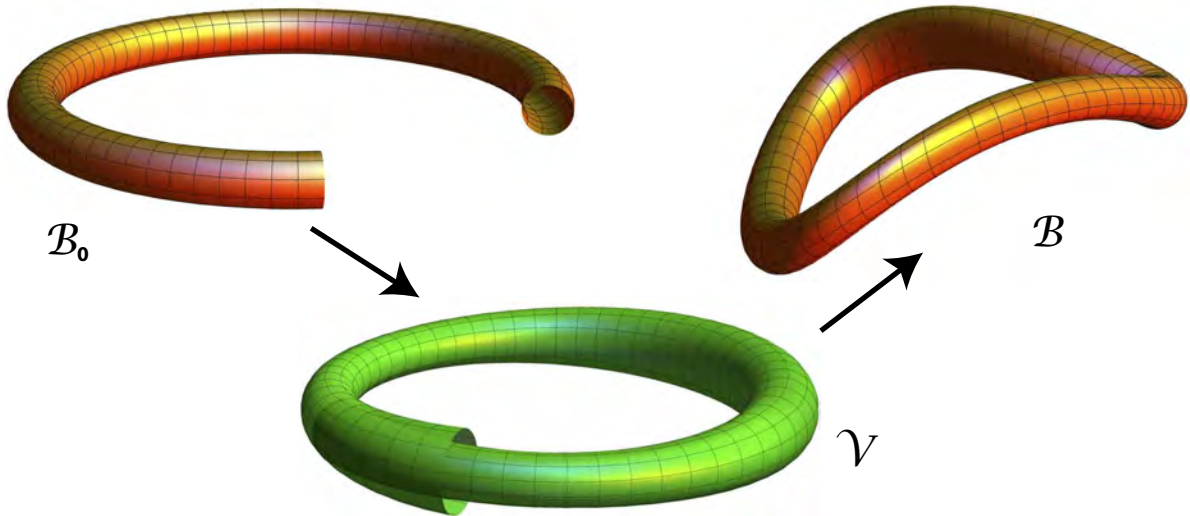


Figure 3: Schematic of the 3 configurations, initial \mathcal{B}_0 , reference \mathcal{V} , and current \mathcal{B} . The reference configuration is stress-free and evolves in time and reflects the change due to growth (shown here, initially the rod has intrinsic curvature; as growth proceeds the cross-section is allowed to grow inhomogeneously and the length of the rod increases). The reference configuration can also intersect itself as it does not represent a possible realization of the rod; rather, it defines its local properties. The current configuration is the actual configuration with correct boundary conditions (here periodic boundary conditions) and body loads.

3.2. Mechanics of a growing rod

At time t , the balance of force and moment in the reference configuration yields

$$\frac{\partial \mathbf{n}}{\partial S} + \mathbf{f} = 0, \quad (36)$$

$$\frac{\partial \mathbf{m}}{\partial S} + \frac{\partial \mathbf{r}}{\partial S} \times \mathbf{n} + \mathbf{l} = 0, \quad (37)$$

where \mathbf{f} and \mathbf{l} are the body force and couple per unit *reference* length. The reference arc length S is the natural choice to express all quantities as the constitutive equations are given in the reference configuration. This equation together with the appropriate boundary conditions and with one of the two constitutive models proposed (either (28) for inextensible rods or (33) for extensible rods) can be solved to obtain the current configuration. We define α to be the *elastic stretch* and λ the *total stretch* between the initial and current configuration. We have

$$\lambda = \alpha\gamma \iff \frac{\partial s}{\partial S_0} = \frac{\partial s}{\partial S} \frac{\partial S}{\partial S_0}. \quad (38)$$

A change of independent variable leads to an alternative formulation in the current and initial configuration. Namely, we have

$$\frac{\partial \mathbf{n}}{\partial s} + \alpha^{-1} \mathbf{f} = 0, \quad (39)$$

$$\frac{\partial \mathbf{m}}{\partial s} + \frac{\partial \mathbf{r}}{\partial s} \times \mathbf{n} + \alpha^{-1} \mathbf{l} = 0, \quad (40)$$

where $\alpha^{-1} \mathbf{f}$ and $\alpha^{-1} \mathbf{l}$ are now the body force and couple per unit *current* length. Finally, in the initial configuration, we have

$$\frac{\partial \mathbf{n}}{\partial S_0} + \gamma \mathbf{f} = 0, \quad (41)$$

$$\frac{\partial \mathbf{m}}{\partial S_0} + \frac{\partial \mathbf{r}}{\partial S_0} \times \mathbf{n} + \gamma \mathbf{l} = 0, \quad (42)$$

where $\gamma \mathbf{f}$ and $\gamma \mathbf{l}$ are the body force and couple per unit *initial* length.

3.3. Constitutive and evolution laws for a single growing rod

Following our assumptions, at the constitutive level and at any given time t the rod is still characterised by one of the three constitutive models described in Section 2.3. Since both reference arc length and stretch can change at time t , great care must be exercised to ensure that these changes in length are correctly taken into account. We advocate the simple principle of always defining first all material properties in the reference configuration \mathcal{V} with respect to the arc length S . All other formulations of the rod equations follow directly from a change of independent variables as shown above. Note that the parameters entering the constitutive equations (stiffnesses and unstressed curvatures) may also evolve in the slow time t .

3.4. Evolution law for a growing rod

We now consider a possible law for the evolution of unstressed curvature. We first consider the case of an inextensible rod. In this case, the only material and structural parameters (possibly function of the position S) evolving in time are the radius, density, stiffness matrix \mathbf{K} and unstressed Darboux vector. Again we assume that S is the arc length in the virtual (grown) configuration. Whereas radii, density, and stiffnesses are quantities whose evolution must be prescribed from biological laws, the unstressed curvatures $\hat{\mathbf{u}}$ depends both on intrinsic quantities and on the geometry of the deformation. To understand this dependence, we adapt the reasoning of [84] to the present terminology and to the three-dimensional case. First, we consider an inner rod with uniform unstressed curvatures $\hat{\mathbf{u}}_{\text{in}}$ and stiffness matrix \mathbf{K}_{in} . Next, we apply a moment so that the new shape has uniform curvatures $\hat{\mathbf{u}}_{\text{out}}$. In this new configuration, we add an external outer cylindrical layer with the present curvature and bending stiffness \mathbf{K}_{out} . Ignoring the possibility of internal residual stresses in the material and treating this new structure as an elastic rod, the problem is to determine its new properties, that is, its curvature $\hat{\mathbf{u}}$ and stiffness matrix \mathbf{K} . For any uniform shape given by \mathbf{u} , the total moment of the composite rod is $\mathbf{K}(\mathbf{u} - \hat{\mathbf{u}})$, which is also equal to the sum of both moments due to the inner and outer rods, so that we have

$$\mathbf{K}_{\text{in}}(\mathbf{u} - \hat{\mathbf{u}}_{\text{in}}) + \mathbf{K}_{\text{out}}(\mathbf{u} - \hat{\mathbf{u}}_{\text{out}}) = \mathbf{K}(\mathbf{u} - \hat{\mathbf{u}}) \quad (43)$$

which must be valid for all \mathbf{u} so that we have both

$$\mathbf{K} = \mathbf{K}_{\text{in}} + \mathbf{K}_{\text{out}}, \quad (44)$$

and

$$\hat{\mathbf{u}} = \mathbf{K}^{-1} (\mathbf{K}_{\text{in}} \hat{\mathbf{u}}_{\text{in}} + \mathbf{K}_{\text{out}} \hat{\mathbf{u}}_{\text{out}}). \quad (45)$$

It is now possible to treat this effect as a continuous process. Consider a deformed rod and assume that at time t it has curvatures $\mathbf{u}(t)$, and material properties $\hat{\mathbf{u}}(t)$ and $\mathbf{K}(t)$. At time $t + \Delta t$, a small new layer is applied to the rod. The balance of moment now reads

$$\mathbf{K}(t)[\mathbf{u}(t + \Delta t) - \hat{\mathbf{u}}(t) - \mathbf{k}_2(t)\Delta t] + \Delta \mathbf{K}[\mathbf{u}(t + \Delta t) - \mathbf{u}(t) - \mathbf{k}_1(t)] = \mathbf{K}(t + \Delta t)[\mathbf{u}(t + \Delta t) - \hat{\mathbf{u}}(t + \Delta t)], \quad (46)$$

where $\Delta \mathbf{K} = \dot{\mathbf{K}}\Delta t$ is the bending stiffness of the new layer, $\mathbf{k}_1(t)$ is the difference between the curvatures of the new layer and the curvatures of the inner rod and $\mathbf{k}_2(t)$ is a source term for the intrinsic curvature of the inner structure. By expanding all quantities to order Δt , we obtain

$$\dot{\mathbf{K}}(\mathbf{u} - \hat{\mathbf{u}} + \mathbf{k}_1) = \mathbf{K}(\dot{\mathbf{u}} - \mathbf{k}_2). \quad (47)$$

If there is no increase of mass or change of stiffness in the section, we have $\dot{\mathbf{K}} = 0$ and the evolution of the curvatures is simply governed by $\dot{\mathbf{u}} = \mathbf{k}_2$ and a choice for \mathbf{k}_2 must be made. For instance, in the plane, the only non-zero component of the curvatures is the Frenet curvature $\kappa = \mathbf{u}_2$. If we assume that the intrinsic curvature relaxes to the current curvature with a relaxation time η^{-1} , we have

$$\dot{\hat{\kappa}} = \eta(\kappa - \hat{\kappa}). \quad (48)$$

This is exactly the law used in [39] to describe the slow evolution of tendrils in climbing plants. We utilize this law in the buckling of a ring in Section 6.1.1 below.

4. A growing rod on a foundation

Of key importance in growing filamentary structures is the development of stresses and buckling instabilities due to external forces. Here we consider a growing rod attached to a rigid foundation via an elastic force, and explore the effect of the induced body force \mathbf{f} and body couple \mathbf{l} . We assume that the foundation is a rigid space curve to which the rod is adhered via a restoring body force dependent solely upon the distance from the rod to the curve. The governing equations of the rod are unchanged; the key is to appropriately capture the body force and body couple generated by attachment to the foundation. To do so, we must first specify the details of the attachment, e.g. where on the rod the force acts, and in which direction. The geometric attachment of a rod of current length l on a foundation of length \hat{l} is specified by a pair of functions $\phi : [0, l] \rightarrow [0, 2\pi[$ and $\mathcal{A} : [0, l] \rightarrow [0, \hat{l}]$ defined as follows

1. The function ϕ defines the material position on the surface of the rod where the attachment occurs. As before, let the centreline of the rod be described in the current configuration by the space curve $\mathbf{r}(s)$. Recall that the cross section is spanned by the vectors \mathbf{d}_1 and \mathbf{d}_2 . The attachment location on the material cross section can be described by a function $\phi(s)$, the angle from the \mathbf{d}_1 axis at which the attachment occurs, so that the rod is attached at the point

$$\mathbf{r}_{\mathcal{A}}(s) = \mathbf{r} + a(\phi(s), s) [\cos(\phi(s)) \mathbf{d}_1 + \sin(\phi(s)) \mathbf{d}_2] \quad (49)$$

where the function $a(\phi(s), s)$ defines the shape of the cross section at $\mathbf{r}(s)$ as a polar function.

2. The function \mathcal{A} defines the location on the foundation to which each point is adhered, i.e. a map between the centreline of the rod and the foundation curve. Let the space curve $\boldsymbol{\rho}(\hat{s})$ describe the foundation. We define the attachment map $\mathcal{A}(s)$ as a one-to-one map from the rod to the foundations such that $\hat{s} = \mathcal{A}(s)$, $\mathcal{A}(0) = 0$ and describing the respective material position where the rod is attached, that is the point $\mathbf{r}_{\mathcal{A}}(s)$ is attached to the point $\boldsymbol{\rho}(\mathcal{A}(s))$.

The situation is depicted in Figure 4. The two functions ϕ and \mathcal{A} as well as the foundation curve $\boldsymbol{\rho}$ define completely the geometry of attachment. We now describe the mechanical force connecting the curve to the rod. We define the “spring vector”² as the vector from the rod to the curve

$$\mathbf{E} = \boldsymbol{\rho}(\mathcal{A}(s)) - \mathbf{r}_{\mathcal{A}}(s), \quad (50)$$

²while we use the word spring for visual and schematic purposes, we do not intend this to mean individual, discrete springs. The reader should keep in mind a continuum of springs, or an elastic sheet.

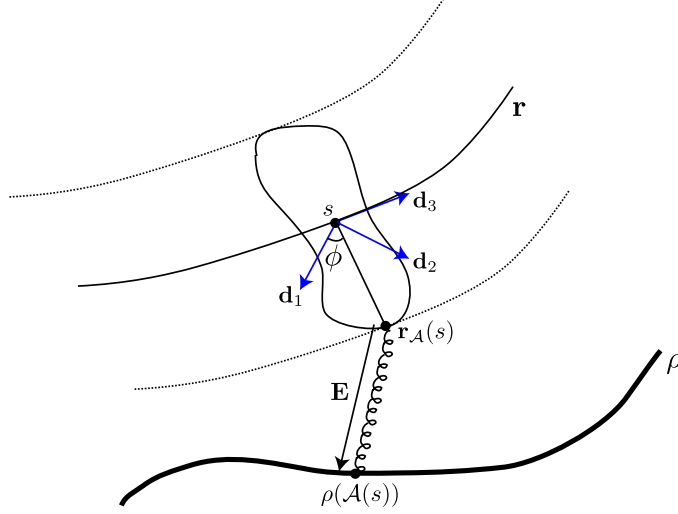


Figure 4: Setup for rod on a foundation. The point \mathbf{r}_A , located on the edge of the rod, is attached to a rigid foundation $\boldsymbol{\rho}$ by an elastic force directed along \mathbf{E} . Since the force does not act on the centreline, a body couple can also be induced.

and assume that the body force generated by the rigid foundation is along that direction, and only depends on the distance relative to a rest length,

$$\mathbf{f}(s) = f(|\mathbf{E}| - q(s)) \frac{\mathbf{E}}{|\mathbf{E}|}, \quad (51)$$

where $q(s)$ is the rest length of the spring, so that $f(0) = 0$ when $|\mathbf{E}| = q$. We further assume that f derives from a convex potential for which the origin is a minimum. The particular case where f is linear corresponds to the classical case of a Winkler foundation with a Hookean spring. Note that in this formulation, no force is generated by shearing the “springs,” i.e. a translation of the rod in which $|\mathbf{E}|$ does not change. This potentially undesirable feature can be removed by introducing a twist force to the foundation, or more simply, by defining $\boldsymbol{\rho}$ so that the rest length $q = 0$.

Since the foundation is attached to the edge of the rod, the force is applied at the edge as opposed to the centreline, and thus the attachment also generates a body couple that is dependent upon the attachment function ϕ and is given by

$$\mathbf{l} = (\mathbf{r}_A - \mathbf{r}) \times \mathbf{f}. \quad (52)$$

A simple example illustrating the effect and generation of a body couple is provided in Appendix A.

5. Buckling criterion

A primary focus in this paper is to study buckling of growing rods. Here we derive a general formulation to determine a buckling criterion of a rod with arbitrary body force and couple. Our starting point is the full kinematic and mechanics description for an unshearable rod, expressed in the reference configuration:

$$\begin{aligned} \frac{\partial \mathbf{r}}{\partial S} &= \alpha \mathbf{d}_3, \\ \frac{\partial \mathbf{d}_i}{\partial S} &= \mathbf{u} \times \mathbf{d}_i, \quad i = 1, 2, 3, \\ \frac{\partial \mathbf{n}}{\partial S} + \mathbf{f} &= 0, \\ \frac{\partial \mathbf{m}}{\partial S} + \frac{\partial \mathbf{r}}{\partial S} \times \mathbf{n} + \mathbf{l} &= 0, \end{aligned} \quad (53)$$

along with the constitutive equations

$$\begin{aligned}\mathbf{m} &= EI_1(u_1 - \hat{u}_1)\mathbf{d}_1 + EI_2(u_2 - \hat{u}_2)\mathbf{d}_2 + \mu J(u_3 - \hat{u}_3)\mathbf{d}_3, \\ n_3 &= EA(\alpha - 1).\end{aligned}\tag{54}$$

Let the rod have constant intrinsic curvature $\hat{\mathbf{u}}$, and suppose that for given growth γ , we have a known solution given by $\mathbf{r}^{(0)}$, $\mathbf{n}^{(0)}$, $\mathbf{u}^{(0)}$, $\mathbf{d}_i^{(0)}$ $i=1,2,3$, and with elastic stretch $\alpha^{(0)}$. The general idea is to add to this solution a small perturbation and determine the critical growth value $\gamma = \gamma^*$ at which a non-trivial solution to the perturbed system exists.

5.1. The perturbation expansion

Let ϵ be a small parameter. Based on the general ideas outlined in [103, 1, 104, 105], we begin by expanding the basis itself, $\mathbf{d}_i = \mathbf{d}_i^{(0)} + \epsilon \mathbf{d}_i^{(1)} + O(\epsilon^2)$. If we express the correction terms $\mathbf{d}_i^{(1)}$ in terms of the unperturbed basis, and require orthonormality to $O(\epsilon)$, we find that the $O(\epsilon)$ corrections can be expressed in terms of a single vector $\mathbf{c} = c_1 \mathbf{d}_1^{(0)} + c_2 \mathbf{d}_2^{(0)} + c_3 \mathbf{d}_3^{(0)}$ such that $\mathbf{d}_i = \mathbf{d}_i^{(0)} + \epsilon \mathbf{c} \times \mathbf{d}_i^{(0)} + O(\epsilon^2)$. We now expand all quantities, such that the first order perturbation of all vector quantities is expressed in the frame $\{\mathbf{d}_i^{(0)}\}$. Generally, for a vector $\mathbf{v} = v_1 \mathbf{d}_1 + v_2 \mathbf{d}_2 + v_3 \mathbf{d}_3$, we write

$$\mathbf{v} = \sum_i (v_i^{(0)} + \epsilon v_i^{(1)}) \mathbf{d}_i^{(0)} + O(\epsilon^2).\tag{55}$$

Note the following relationship: if, alternatively, we were to expand each $v_i = v_i^{(0)} + \epsilon v_i^{(1)}$, we would have $v_i^{(0)} = \mathbf{v}_i^{(0)}$ and $v_i^{(1)} = \mathbf{v}_i^{(1)} - (\mathbf{c} \times \mathbf{v}^{(0)})_i$, where $\mathbf{v}^{(0)} = \sum_i v_i^{(0)} \mathbf{d}_i^{(0)}$. We expand \mathbf{r} , \mathbf{n} , and \mathbf{u} in this fashion, and also $\alpha = \alpha^{(0)} + \epsilon \alpha^{(1)} + O(\epsilon^2)$. We assume that the body force \mathbf{f} and body couple \mathbf{l} can be expanded similarly.

Inserting these expansions into Equations (53) and (54), we obtain a linear system for the 13 independent variables $\{r_1^{(1)}, r_2^{(1)}, r_3^{(1)}, n_1^{(1)}, n_2^{(1)}, n_3^{(1)}, u_1^{(1)}, u_2^{(1)}, u_3^{(1)}, c_1^{(1)}, c_2^{(1)}, c_3^{(1)}, \alpha^{(1)}\}$. The force balance reads ($' = \frac{\partial}{\partial S}$)

$$(n_1^{(1)})' = u_3^{(0)} n_2^{(1)} - u_2^{(0)} n_3^{(1)} + f_1^{(1)}\tag{56}$$

$$(n_2^{(1)})' = u_1^{(0)} n_3^{(1)} - u_3^{(0)} n_1^{(1)} + f_2^{(1)}\tag{57}$$

$$(n_3^{(1)})' = u_2^{(0)} n_1^{(1)} - u_1^{(0)} n_2^{(1)} + f_3^{(1)}.\tag{58}$$

The moment balance is

$$\begin{aligned}& EI_1 \left((u_2^{(0)} c_3)' - (u_3^{(0)} c_2)' + (u_1^{(1)})' + (\hat{u}_1 - u_1^{(0)})(u_3^{(0)} c_3 + u_2^{(0)} c_2) \right) + \\& EI_2 \left((\hat{u}_2 - u_2^{(0)}) c_3' - (u_2^{(0)})' c_3 + u_1^{(0)} u_3^{(0)} c_3 + ((u_2^{(0)})^2 - (u_3^{(0)})^2 - u_2^{(0)} \hat{u}_2) c_1 - u_3^{(0)} u_2^{(1)} \right) + \\& \mu J \left((u_3^{(0)} - \hat{u}_3) c_2' + (u_3^{(0)})' c_2 + u_1^{(0)} u_2^{(0)} c_2 + ((u_3^{(0)})^2 - (u_2^{(0)})^2 - u_3^{(0)} \hat{u}_3) c_1 + u_2^{(0)} u_3^{(1)} \right) - \\& \alpha^{(0)} n_3^{(0)} c_1 - \alpha^{(0)} n_2^{(1)} - n_2^{(0)} \alpha^{(1)} + l_1^{(1)} = 0,\end{aligned}\tag{59}$$

$$\begin{aligned}& EI_1 \left((u_1^{(0)} - \hat{u}_1) c_3' + (u_1^{(0)})' c_3 + u_2^{(0)} u_3^{(0)} c_3 + ((u_1^{(0)})^2 - (u_3^{(0)})^2 - u_1^{(0)} \hat{u}_1) c_2 + u_3^{(0)} u_1^{(1)} \right) + \\& EI_2 \left((u_3^{(0)} c_1)' - (u_1^{(0)} c_3)' + (u_2^{(1)})' + (\hat{u}_2 - u_2^{(0)})(u_1^{(0)} c_1 + u_3^{(0)} c_3) \right) + \\& \mu J \left((\hat{u}_3 - u_3^{(0)}) c_1' - (u_3^{(0)})' c_1 + u_1^{(0)} u_2^{(0)} c_1 + ((u_3^{(0)})^2 - (u_1^{(0)})^2 - u_3^{(0)} \hat{u}_3) c_2 - u_1^{(0)} u_3^{(1)} \right) - \\& \alpha^{(0)} n_3^{(0)} c_2 + \alpha^{(0)} n_1^{(1)} + n_1^{(0)} \alpha^{(1)} + l_2^{(1)} = 0,\end{aligned}\tag{60}$$

$$\begin{aligned}& EI_1 \left((\hat{u}_1 - u_1^{(0)}) c_2' - (u_1^{(0)})' c_2 + u_2^{(0)} u_3^{(0)} c_2 + ((u_1^{(0)})^2 - (u_2^{(0)})^2 - u_1^{(0)} \hat{u}_1) c_3 - u_2^{(0)} u_1^{(1)} \right) + \\& EI_2 \left((u_2^{(0)} - \hat{u}_2) c_1' + (u_2^{(0)})' c_1 + u_1^{(0)} u_3^{(0)} c_1 + ((u_2^{(0)})^2 - (u_1^{(0)})^2 - u_2^{(0)} \hat{u}_2) c_3 + u_1^{(0)} u_2^{(1)} \right) + \\& \mu J \left((u_1^{(0)} c_2)' - (u_2^{(0)} c_1)' + (u_3^{(1)})' + (\hat{u}_3 - u_3^{(0)})(u_1^{(0)} c_1 + u_2^{(0)} c_2) \right) + \\& \alpha^{(0)} n_1^{(0)} c_1 + \alpha^{(0)} n_2^{(0)} c_2 + l_3^{(1)} = 0.\end{aligned}\tag{61}$$

The kinematic equation $\frac{\partial \mathbf{r}}{\partial S} = \alpha \mathbf{d}_3$ reads

$$(r_1^{(1)})' + u_2^{(0)} r_3^{(1)} - u_3^{(0)} r_2^{(1)} = \alpha^{(0)} c_2 \quad (62)$$

$$(r_2^{(1)})' + u_3^{(0)} r_1^{(1)} - u_1^{(0)} r_3^{(1)} = -\alpha^{(0)} c_1 \quad (63)$$

$$(r_3^{(1)})' + u_1^{(0)} r_2^{(1)} - u_2^{(0)} r_1^{(1)} = \alpha^{(1)}, \quad (64)$$

and the frame equations $\frac{\partial \mathbf{d}_i}{\partial S} = \mathbf{u} \times \mathbf{d}_i$ take the following simple form at $O(\epsilon)$

$$c_1' = u_1^{(1)}, \quad c_2' = u_2^{(1)}, \quad c_3' = u_3^{(1)}. \quad (65)$$

In the case of an inextensible rod, $\alpha^{(0)} = 1$ and $\alpha^{(1)} = 0$, while for an extensible rod the constitutive equation (34) gives

$$n_3^{(1)} + n_1^{(0)} c_2 - n_2^{(0)} c_1 = EA \alpha^{(1)}. \quad (66)$$

5.2. Bifurcation criterion

To obtain a bifurcation criterion, we define the 9 dimensional vector

$$\boldsymbol{\mu} = \{r_1^{(1)}, r_2^{(1)}, r_3^{(1)}, n_1^{(1)}, n_2^{(1)}, n_3^{(1)}, c_1^{(1)}, c_2^{(1)}, c_3^{(1)}\}. \quad (67)$$

Note that we can eliminate the $u_i^{(1)}$ immediately using (65), and $\alpha^{(1)}$ using (66). The system can be written in compact matrix form

$$\mathbf{M}_2 \boldsymbol{\mu}'' + \mathbf{M}_1 \boldsymbol{\mu}' + \mathbf{M}_0 \boldsymbol{\mu} = \mathbf{0}, \quad (68)$$

where each \mathbf{M}_i is a constant matrix depending on the solution at first order. We then look for a solution of the form $\boldsymbol{\mu} = \boldsymbol{\xi} e^{inS/\gamma} + \bar{\boldsymbol{\xi}} e^{-inS/\gamma}$. Inserting this form into (68), the system is satisfied if $\det \mathbf{M} = 0$, where

$$\mathbf{M} = \mathbf{M}(\gamma; n) = -n^2 \mathbf{M}_2 + in \mathbf{M}_1 + \mathbf{M}_0. \quad (69)$$

The critical growth γ^* is the smallest value of $\gamma > 1$, minimised over n , at which the determinant vanishes, and the corresponding value of n determines the mode or wavelength of the buckling, depending on the particular geometry.

6. Growing rings

A classic problem in the theory of elastic rods is the buckling of a ring to a non-circular shape. This problem was first considered by Michell in 1889 [106, 107] for the case of a twisted ring. Similarly, the problem of the stability of a ring with intrinsic curvature under a variety of loadings and material parameters has been considered by many authors [108, 109, 110, 111, 112] and is known to be relevant for the study of DNA mini-rings [113, 114, 115, 93].

Here, we use this simple configuration to demonstrate the relative effects of growth, remodeling, and an elastic foundation on the buckling and shape of rods. We consider an inextensible ring of initial and unstressed radius 1, with cross-sectional radius a . We assume that it grows linearly in time so that $\gamma = 1 + mt$ while keeping all other material properties unchanged. We can set, without loss of generality, $m = 1$ by rescaling t , which is now the growth time. In this case, we have $\hat{\mathbf{u}} = (0, 1, 0)$, $L = 2\pi\gamma$.

6.1. Without external force

First we study the buckling of the growing ring in the absence of external forces. In the absence of remodeling the buckling is strictly determined by the critical γ . For this system there exists for all $\gamma \geq 1$ circular solutions characterised by curvature $u_2 = 1/\gamma$, vanishing force $\mathbf{n} = 0$, and maintained by a bending moment $\mathbf{m} = EI(u_2 - 1)$ generated by the periodic boundary condition (the condition that the cross sections at $s = 0$ and $s = L$ agree perfectly). Let the ring be situated in the x - y plane, and with Frenet basis

$$\mathbf{d}_1^{(0)} = -\cos(S/\gamma) \mathbf{e}_x - \sin(S/\gamma) \mathbf{e}_y, \quad \mathbf{d}_2^{(0)} = \mathbf{e}_z, \quad \mathbf{d}_3^{(0)} = -\sin(S/\gamma) \mathbf{e}_x + \cos(S/\gamma) \mathbf{e}_y. \quad (70)$$

Then the initial solution is described by $r_1^{(0)} = -\gamma$, $u_2^{(0)} = 1/\gamma$, with all other quantities equal to zero. Inserting this into Equations (56) - (65), the determinant condition can be solved explicitly for γ , and is found to be

$$\gamma(n) = \frac{1 - \Gamma + \sqrt{1 + (4n^2 - 2)\Gamma + \Gamma^2}}{2}, \quad (71)$$

where Γ is given by (32) and the buckling mode n must be an integer to satisfy the periodic boundary conditions of the closed ring. The critical growth is the smallest value of $\gamma > 1$, which occurs at $n = 2$.

6.1.1. Remodeling

In this section we incorporate remodeling of the ring. The basic question is: if the intrinsic curvature of the ring evolves such that it relaxes to the current curvature with a particular relaxation time, does the ring still buckle? In the previous section, the rate of growth was unimportant, the buckling was dictated purely by the amount of growth. Here, whether or not the ring buckles and when, depends on a competition between the growth rate and the relaxation rate.

In the growth process, let the unstressed curvature evolve to the current curvature following the law (48) (so that if growth is interrupted, the ring evolves to an unstressed state with a characteristic time $1/\eta$). As long as the central axis of the rod remains circular, the curvature is, as before, $u_2 = 1/\gamma = 1/(1+t)$, which can be used directly in (48), so that

$$\frac{\partial \hat{u}_2}{\partial t} = \eta \left(\frac{1}{1+t} - \hat{u}_2 \right). \quad (72)$$

The solution of this last equation can be expressed in terms of the exponential integral $\text{Ei}(\cdot)$ as

$$\hat{u}_2(t) = e^{-\eta(1+t)} [e^\eta + \eta \text{Ei}(\eta(1+t)) - \eta \text{Ei}(\eta)]. \quad (73)$$

The buckling criterion is found in the same way as in the previous section, but now must be computed in terms of the critical time, as \hat{u}_2 is not a fixed constant; we now have a competition between the growth of the ring and the remodeling of the unstressed curvature. Here, the ring becomes unstable when

$$\frac{u_2}{\hat{u}_2} \leq c \equiv \frac{\Gamma - 1 + \sqrt{\Gamma^2 + 14\Gamma + 1}}{8\Gamma}, \quad (74)$$

at which time, the solution does not remain planar and the expression for the intrinsic curvature (73) ceases to be valid. The evolution of u_2/\hat{u}_2 is plotted in Figure 5 for various values of η . If the relaxation rate is high enough, the criterion (74) is never satisfied and the ring never buckles. In this situation where we have two dynamical processes, the history of the deformation has to be taken into account. A similar situation for the Euler buckling of a straight rod and the twisted ring has been discussed in [39, 87].

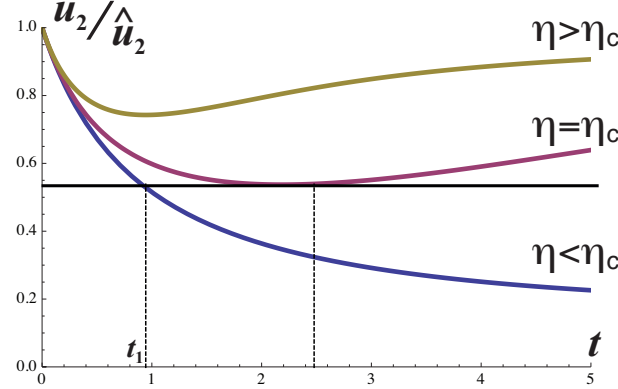


Figure 5: Stability of growing ring with evolving unstressed curvature. For illustrative purpose we chose $\Gamma = 3/4$, which leads to the condition ~ 0.54 , for $\eta < \eta_c \sim 0.57$, the instability occurs at time t_1 whereas for $\eta > \eta_c$, the unstressed curvature evolves sufficiently fast as to remove stresses in the ring and no instability takes place (upper curve: $\eta = 2$, lower curve $\eta = 0.1$).

6.1.2. Post buckling regime

Equation (71) provides the critical point at which the ring buckles. Next we consider the solution after buckling and without remodeling, and highlight its intricate mathematical structure. A full numerical solution for the post buckled ring can be obtained by solving the full system via a shooting method [116] and parameter continuation. This solution is shown in Figure 6. Note that we have not taken into account self-contact. Nevertheless, the ring follows an interesting deformation path. By $\gamma \approx 2.19$, the closed rod has collapsed back into a planar ring, tripled on itself. As γ continues to increase, this tripled ring grows, so that at $\gamma = 3$, it forms a tripled ring of radius 1. At this point, the curvature everywhere matches the intrinsic

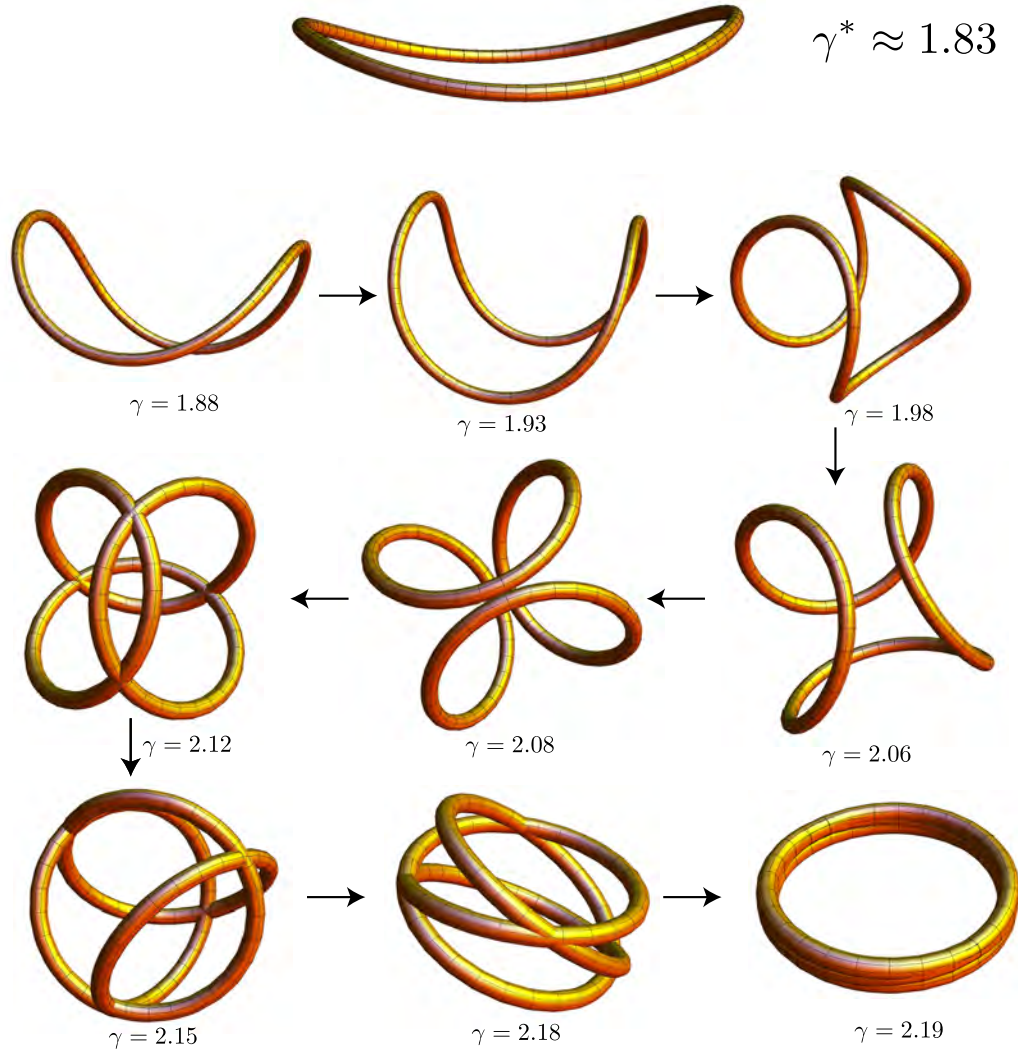


Figure 6: The shape of a growing ring after buckling, computed from a numerical analysis with $\Gamma = 0.7$.

curvature; the ring has resolved back to a stress-free state. Through a numerical linear stability analysis, we have verified that the solutions throughout the deformation are in fact stable.

What happens if the tripled ring continues to grow? The same buckling analysis as above can be performed to determine when the tripled ring will buckle if we further increase γ . The difference is that now the length of the rod is three times the radius. Thus the buckling mode n in Equation (71) does not have to be an integer, but rather an integer multiple of $1/3$. The “second buckling” occurs at $\gamma \approx 3.83$, and corresponds to mode $4/3$. This solution is plotted on the right side of Figure 8. Interestingly, mode $2/3$ occurs for $\gamma \approx 2.18$, and has the same form as the post buckled ring in Figure 6 just before collapsing back into the planar tripled ring. For comparison, studies of various multicovered rings can be found in [117, 112, 104].

6.1.3. Fourier modes for the buckled ring

The periodicity of the problem invites a Fourier analysis. Moreover, the numerical solution suggests that the buckled ring can be approximated by expressions depending on a few Fourier modes only. We therefore derive an approximate, low dimensional model to yield analytical solutions.

Applying (36,37) to the case of this inextensible ($\frac{\partial \mathbf{r}}{\partial S} = \mathbf{d}_3$) ring gives:

$$\begin{aligned}\frac{\partial \mathbf{n}}{\partial S} &= 0, \\ \frac{\partial \mathbf{m}}{\partial S} + \mathbf{d}_3 \times \mathbf{n} &= 0.\end{aligned}\tag{75}$$

Numerical analysis indicates that both the planar and buckled solutions satisfy $\mathbf{n} = 0$. Equation (75) therefore reduces to $\frac{\partial \mathbf{m}}{\partial S} = 0$ with the constitutive relation $\mathbf{m} = EI(\mathbf{u}_1 \mathbf{d}_1 + (\mathbf{u}_2 - \hat{\mathbf{u}}_2) \mathbf{d}_2 + \Gamma \mathbf{u}_3 \mathbf{d}_3)$, and the definition $\frac{\partial \mathbf{d}_i}{\partial S} = \mathbf{u} \times \mathbf{d}_i$. Projecting the moment balance equation in the local basis $\{\mathbf{d}_i\}$, and rescaling $S = \gamma S^*/\hat{u}_2$ and $\mathbf{u}_i = \hat{u}_2 \mathbf{u}_i^*$ yields:

$$\begin{aligned}\frac{1}{\gamma} \frac{d\mathbf{u}_1^*}{dS^*} &= (1 - \Gamma) \mathbf{u}_2^* \mathbf{u}_3^* - \mathbf{u}_3^*, \\ \frac{1}{\gamma} \frac{d\mathbf{u}_2^*}{dS^*} &= -(1 - \Gamma) \mathbf{u}_1^* \mathbf{u}_3^*, \\ \frac{\Gamma}{\gamma} \frac{d\mathbf{u}_3^*}{dS^*} &= \mathbf{u}_1^*,\end{aligned}\tag{76}$$

where the choice of parameterization S^* lets the growth factor appear explicitly. The system (76) possesses two invariants: $\frac{d}{dS^*}(\mathbf{u}_1^{*2} + \mathbf{u}_2^{*2} + \Gamma \mathbf{u}_3^{*2}) = 0$ and $\frac{d}{dS^*}(\mathbf{u}_2^* + \Gamma \frac{1-\Gamma}{2} \mathbf{u}_3^{*2}) = 0$. Its solution therefore lies on a closed loop in the $\{\mathbf{u}_1^*, \mathbf{u}_2^*, \mathbf{u}_3^*\}$ space at the intersection of an ellipsoid and a cylindrical paraboloid as can be seen in Figure 7. The periodic orbit lying on the intersection can be characterised in terms of its Fourier modes and an approximate model of (76) in terms of the first few non-trivial Fourier modes can be obtained. Indeed

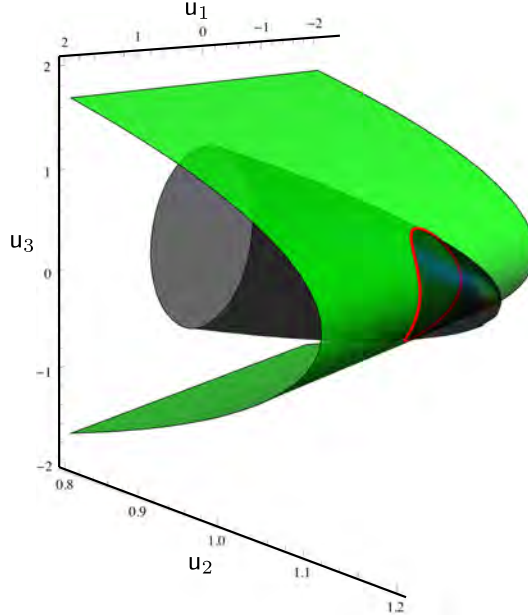


Figure 7: The solution of (76) lies at the intersection (red) of an ellipsoid (black) and a cylindrical paraboloid (green): $\mathbf{u}_1^{*2} + \mathbf{u}_2^{*2} + \Gamma \mathbf{u}_3^{*2} = R^2$ and $\mathbf{u}_2^* + \Gamma \frac{1-\Gamma}{2} \mathbf{u}_3^{*2} = A$. The figure shows the case $\gamma = 2.03$ and $\Gamma = 0.7$. As shown in the Appendix, the constants can be found a posteriori using the solution (139) together with the value of ρ_3 at which the determinant of the system (153) vanishes.

we show in Appendix B that one can reduce the problem of finding the shape of the ring after bifurcation to finding the root of a polynomial equation of degree 4 in the (square of the) amplitude of the leading Fourier mode of \mathbf{u}_3^* . Once the root is obtained, the solution can be reconstructed as shown in Figure 8.

6.2. Growing ring on a foundation

Next we attach the growing ring to a foundation, and in particular analyse the effect on the buckling. We consider two possible configurations for the foundation.

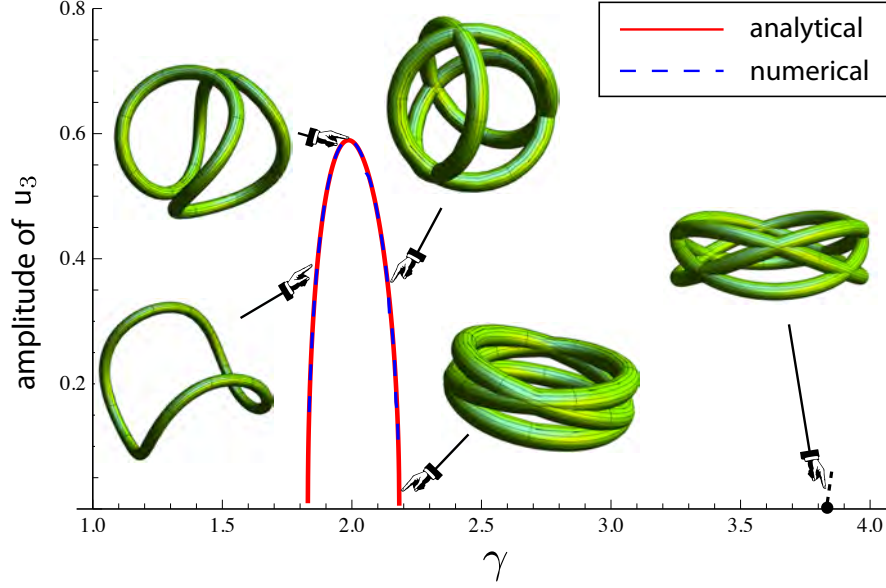


Figure 8: Comparison between the amplitude of u_3^* obtained from the numerical simulation (blue) for $\Gamma = 0.7$ and the value predicted by the low dimensional model (red).

6.2.1. Foundation inside

First we consider the case in which the foundation is attached to the inside edge of the ring in its initial unstressed state. As the ring grows, the foundation exerts an increasing elastic force directed towards the centre of the ring. To compute the circular, prebuckled solution, we again let the ring be located in the x - y plane and let the initial frame $\{\mathbf{d}_i^{(0)}\}$ be given by (70). The foundation is attached at the point $\mathbf{r}_A = \mathbf{r} + a\mathbf{d}_1$, where a is the cross-sectional radius of the rod, and we assume the foundation generates a linear force,

$$\mathbf{f} = k(\boldsymbol{\rho} - \mathbf{r}_A), \quad (77)$$

where the foundation $\boldsymbol{\rho}$ is a circle of radius $1 - a$, located in the x - y plane and centred at the origin. Note also the associated couple given by (52). The circular solution (see Figure 9) has centreline $r_1^{(0)} = -\gamma$, $r_2^{(0)} = r_3^{(0)} = 0$. Since $\boldsymbol{\rho} = -(1 - a)\mathbf{d}_1^{(0)}$, it follows that $f_1^{(0)} = k(\gamma - 1)$, with $f_2^{(0)} = f_3^{(0)} = 0$, and all $l_i^{(0)} = 0$. As before, $u_2^{(0)} = 1/\gamma$, and now the foundation force is balanced by an axial force $n_3^{(0)} = -k\gamma(\gamma - 1)$.

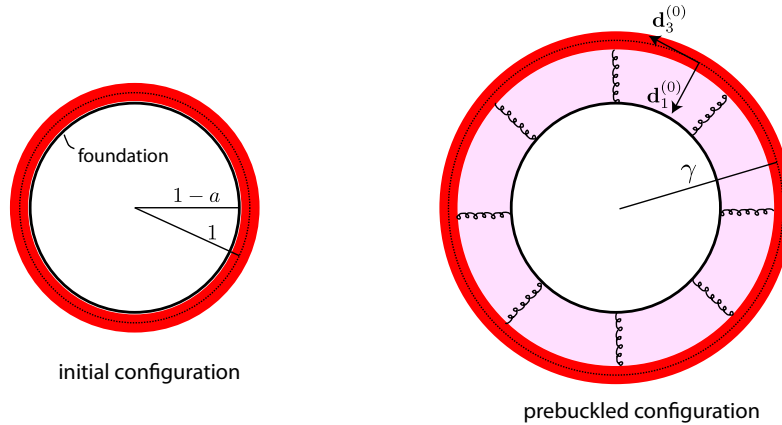


Figure 9: Circular solution for the growing ring with foundation on inside edge, viewed from above. Lengths are scaled by $1/\hat{u}_2$.

To compute the critical growth, the body force (77) and couple (52) are expanded to $O(\epsilon)$, yielding

$$f_1^{(1)} = -kr_1^{(1)}, \quad f_2^{(1)} = -k(r_2^{(1)} + a\mathbf{c}_3), \quad f_3 = -k(r_3^{(1)} - a\mathbf{c}_2), \quad (78)$$

$$l_1^{(1)} = 0, \quad l_2^{(1)} = -a(f_3^{(1)} + \mathbf{c}_2 f_1^{(0)}), \quad l_3^{(1)} = a(f_2^{(1)} - \mathbf{c}_3 f_1^{(0)}). \quad (79)$$

Following Section 5, these expressions are inserted into the system of Equations (56) - (65), and a determinant condition is formed for the critical growth γ^* . The result, and the general effect of the foundation on the buckling, is illustrated in Figure 10, in which γ^* is plotted against the log of the foundation stiffness k for modes $n = 2, 3, 4$. For small k , the solution is similar to the case of no foundation: the ring buckles at mode 2, and as $k \rightarrow 0$, the buckling criterion (71) is recovered. As the stiffness is increased, the critical growth decreases (i.e. the ring buckles earlier), as might be expected. At the same time, the buckling mode n increases. That is, as the foundation force strengthens, it becomes energetically favourable to buckle at higher mode, solutions which have higher bending energy but remain closer to the foundation.

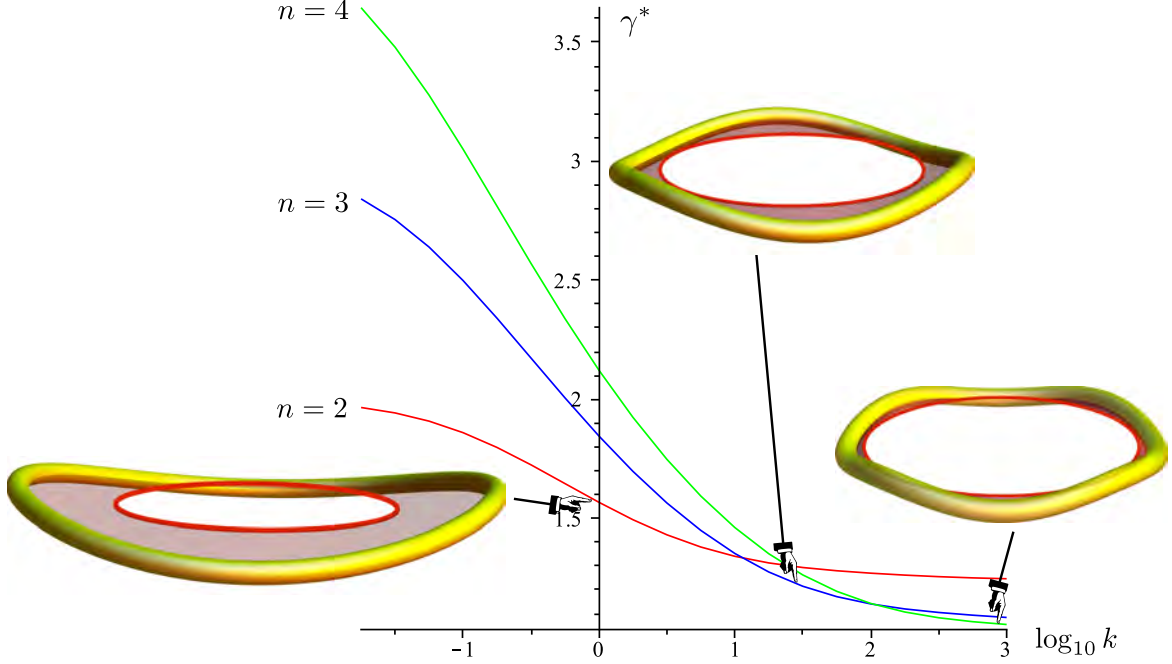


Figure 10: Critical buckling growth plotted against the log of the foundation stiffness k , for modes 2,3, and 4. As the stiffness increases, the buckling occurs after less growth, and at higher modes. The diagram is plotted for $\Gamma = 1$ and $a\bar{u}_2 = 0.07$.

6.2.2. Foundation underneath

Next we consider the alternative configuration in which the foundation lies under the ring in its initial unstressed state. In this configuration, any growth of the ring induces not just a body force, but also a body couple (with the foundation attached to the bottom of the ring, as the ring expands the foundation induces a moment that serves to twist the ring and roll its centreline into the plane of the foundation, see Figure 11). Thus, there is a non-zero register angle φ , i.e. the angle of rotation of the cross section due to the applied couple. Writing the normal and binormal vectors

$$\boldsymbol{\nu} = -\cos(S/\gamma)\mathbf{e}_x - \sin(S/\gamma)\mathbf{e}_y, \quad \boldsymbol{\beta} = \mathbf{e}_z, \quad (80)$$

we have $\mathbf{d}_1^{(0)} = \cos\varphi\boldsymbol{\nu} + \sin\varphi\boldsymbol{\beta}$, $\mathbf{d}_2^{(0)} = -\sin\varphi\boldsymbol{\nu} + \cos\varphi\boldsymbol{\beta}$. Following Equation (18), $u_1^{(0)} = \gamma^{-1}\sin\varphi$, $u_2^{(0)} = \gamma^{-1}\cos\varphi$, $u_3^{(0)} = 0$. The foundation force is of the form (77), but now $\mathbf{r}_A = \mathbf{r} - a\mathbf{d}_2$, and the foundation is a circle of radius 1, located in the x - y plane, i.e. $\boldsymbol{\rho} = -\boldsymbol{\nu}$.

The prebuckled solution has as centreline a circle radius γ , located in the plane $z = h$. Mechanical equilibrium is satisfied if the plane of the ring satisfies $h = a \cos \varphi$, and the register angle solves

$$EI\gamma^{-1} \sin \varphi + ka \cos \varphi (a \sin \varphi - \gamma + 1) = 0. \quad (81)$$

The buckling parameter γ^* is computed similarly as before, with ϕ determined as the root of (81). In Figure

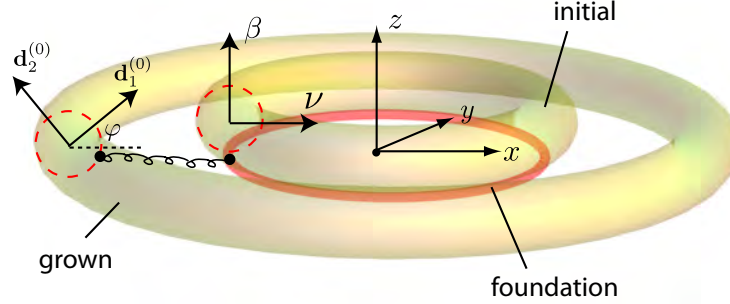


Figure 11: Growing ring with foundation underneath.

12, γ^* is plotted against the log of the foundation stiffness. The general effect of the foundation is similar to the previous section; however, with this setup modes 2 and 3 do not exist for all values of k , and mode 2 has a minimum value. This leads to the interesting difference that the critical growth does not monotonically or even continuously decrease with increasing foundation stiffness. Also of note is that compared to the case of the foundation on the inside edge, the ring with foundation underneath is generally more stable, i.e. buckles for larger γ^* for all values of k . This is due to the induced body couple in the planar state, which serves to counteract the spring force and reduce the internal stress in the rod, thus stabilising slightly compared to the previous case.

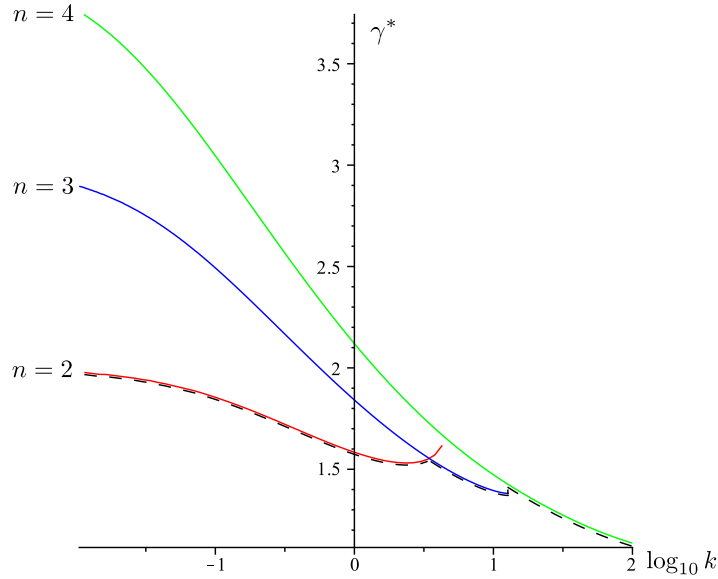


Figure 12: Critical buckling growth in the case of the foundation underneath the initial ring. The dashed line is the envelope of the critical growth – it is not monotonic, and suffers a discontinuous jump in the transition from mode 3 to mode 4. The diagram is plotted for $\Gamma = 1$ and $a\hat{u}_2 = 0.07$.

7. Growing naturally straight rods

Another natural configuration to study is a straight growing filament. A typical approach for these system is to use a (growing) beam on an elastic foundation [69, 70]. However, from a modeling perspective the beam on a foundation lacks crucial features and a distinction between the coordinates and arc length of material points (as material points are labeled by their position along the axis of the beam even during deformation). This can be more confusing if the beam grows or is extensible. Here, we show that the theory of Kirchhoff rod is the natural framework for modeling and studying straight growing filaments on a foundation.

7.1. Uniaxial deformation

We start with the simple problem of an elastic rod being pulled and growing as a response to applied tension. This model is motivated by experiments of growing axons on a substrate, Experiments where one end of the axon is fixed while the other end of the axon is pulled with either constant velocity or constant pulling forces can be performed with high accuracy [118, 119]. The typical range of applied forces is 1-8 nN (nano-Newtons) and the position as a function of time of the axon tip can be measured by standard microscopy. These experiments have revealed that after a critical tension below which no growth occurs, the growth rate is mostly linear with the applied tension [120, 43, 118, 42, 121]. This elongation results from stretching the neurons for long period of time. If, instead, the axon is suddenly “plucked” it will respond quickly depending on its material properties rather than its growth response to external stimuli. On these time scales, the axon was shown to behave mostly like a Hookean spring past a critical rest tension corresponding to the tension in axons in the absence of external loads

From these basic observations, we can model the axon as a one-dimensional rod subject to growth as described before. The filament is of length l and anchored at the growth body at the point $s = 0$ and is only allowed to deform along its length. Following the analysis and the ideas presented in [41, 122], we assume that the tension n_3 in the axon is due to both the applied tension at the end and to an adhesion force between the substrate and the axon. At any given time, we assume that the axon is elastic and operate in small deformation, so that it is characterized by

$$n_3 = E(\alpha - 1). \quad (82)$$

Since there is an adhesion force f acting on the filament due to its interaction with the substrate, the tension along the filament is given by

$$\frac{\partial n_3}{\partial S} + f_3 = 0. \quad (83)$$

We further assume that the adhesion force can be modelled by a simple Hookean law

$$f_3 = k(s(S) - S). \quad (84)$$

Taking an extra derivative of (83) and using the Hookean relationship (82), we obtain

$$\frac{\partial^2 n_3}{\partial S^2} + \frac{n_3}{a^2} = 0, \quad (85)$$

where $a = \sqrt{E/k}$ is a characteristic length for the problem. Since the proximal end of the filament ($s = 0$) remains fixed, $s(0) = 0$, which implies $f_3(0) = 0$ and $\frac{\partial n_3}{\partial S}(0) = 0$. The other end is pulled with a tension $n_3(s = L) = \sigma_L$. The solution of (85) with these boundary conditions is

$$n_3(S(t)) = \sigma_L \frac{\cosh(S(t)/a)}{\cosh(L(t)/a)}. \quad (86)$$

For large a , that is for very small adhesion force or very stiff filament, the tension in the filament becomes uniform ($\lim_{a \rightarrow \infty} n_3(S) = \sigma_L$). For small a , i.e. large adhesion force or very compliant filament, the tension is localized at the side of the pulling with an exponential decay of characteristic length a . In an experiment where the end is pulled with a constant tension σ_L , the behavior of the filament would still appear Hookean as it will extend to a length $l = L + (a/E) \tanh(L/a) \sigma_L$. That is, an extension proportional to the applied tension.

Next, we consider a growth law for the evolution of $S(t)$. At time $t = 0$, the filament of length L_0 is parameterized by its initial arc length S_0 and the change in reference configuration is described by $\gamma = \frac{\partial S}{\partial S_0}$ and a growth law of the form

$$\frac{\partial \gamma}{\partial t} = \gamma g(\mathbf{n}_3). \quad (87)$$

If γ is known, the evolution of a material point initially at position S_0 is given by

$$S(S_0, t) = \int_0^{S_0} \gamma dS_0. \quad (88)$$

That is,

$$\begin{aligned} \partial_t S(S_0, t) &= \int_0^{S_0} (\partial_t \gamma) dS_0 \\ &= \int_0^{S_0} \gamma g(\mathbf{n}_3) dS_0 \\ &= \int_0^S g(\mathbf{n}_3(S)) dS. \end{aligned} \quad (89)$$

Note that since S evolves in time the adhesion given by (84) corresponds to an evolving adhesion. It is an effective phenomenological model for a foundation where attachment and detachment are continuously occurring as the rod slides on the foundation. Hence, it is reminiscent of a viscous drag force. Assuming that growth takes place when the tension is larger than a critical tension σ^* , we have

$$g(\mathbf{n}_3) = \hat{k}(\mathbf{n}_3 - \sigma^*)H(\mathbf{n}_3 - \sigma^*), \quad (90)$$

where $H(\cdot)$ is the Heaviside function. Using the explicit form (86) for the tension, the equation for $S(t)$ is

$$\begin{aligned} \partial_t S &= \hat{k}H(S - S^*) \int_{S^*}^S \left(\sigma_L \frac{\cosh(S/a)}{\cosh(L/a)} - \sigma^* \right) dS \\ &= \hat{k}H(S - S^*) \left[\sigma^*(S^* - S) + a\sigma_L \frac{\sinh(S/a) - \sinh(S^*/a)}{\cosh(L/a)} \right], \end{aligned} \quad (91)$$

where $S^* = a \operatorname{arccosh}(\frac{\sigma^*}{\sigma_L} \cosh \frac{L}{a})$. This last equation gives at any length L the velocity profile as a function of the reference length S at time t , that is

$$V(S, t) = \hat{k}H(S - S^*) \left[\sigma^*(S^* - S) + a\sigma_L \frac{\sinh(S/a) - \sinh(S^*/a)}{\cosh(L/a)} \right]. \quad (92)$$

A typical velocity profile is shown in Figure 13.

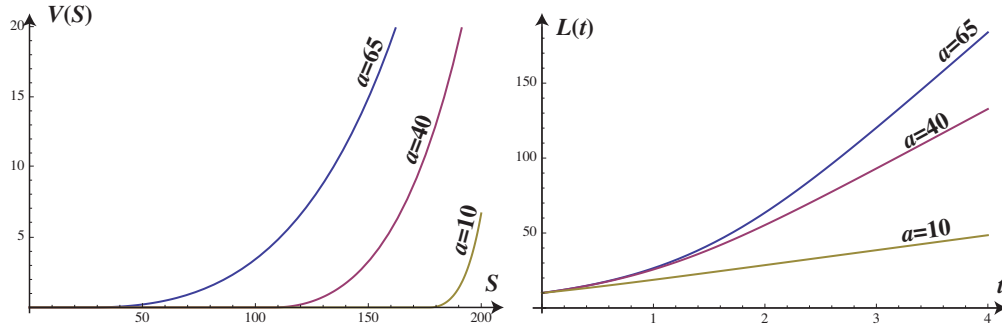


Figure 13: Left: Velocity of points along a growing axon; $L = 200, \sigma_L = 1, \sigma^* = 1/10, k = 1$. Right: Length as a function of time in the limit case where $\sigma^* = 0$, parameters as for the left graph.

Note that Equation (91) for $S(t)$ cannot be solved directly as both S and L depend on t . Therefore, we specialize this equation at the point $S(t) = L(t)$

$$\partial_t L = \hat{k}\sigma^*(S^* - L) + \hat{k}a\sigma_L \frac{\sinh(L/a) - \sinh(S^*/a)}{\cosh(L/a)} \quad (93)$$

with initial conditions $L(t) = L_0$. No useful closed-form solution exists for this equation. Instead, we consider the limit where $\sigma^* \rightarrow 0$ which leads to $\partial_t L = \hat{k} a \sigma_L \tanh(L/a)$, that is

$$L(t) = a \operatorname{arcsinh} \left[e^{\hat{k} \sigma_L t} \sinh(L_0/a) \right]. \quad (94)$$

Once the function $L(t)$ is known, it can be substituted in Eq. (91) and an equation for the evolution of $S(t)$ can be found for all initial points of the form $S(t=0) = S_0$. Note that after an initial exponential phase where the entire filament experiences growth, growth becomes limited to a finite zone close to the tip of characteristic size a and growth becomes linear with time (see Figure 13). Interestingly, the analysis given here based on the growth of the filament and the remodeling of the foundation is equivalent to the analysis given in [122] based on a viscous fluid model for the growth dynamics where it was shown to be consistent with experimental data on axonal growth [118]. In particular, our model correctly predicts that the growth rate of the axon under constant tension asymptotes to a constant value (see $L(t)$ in Fig. 13).

7.2. Planar deformations

The previous example dealt with a rod constrained along a line. Next, we consider the buckling of a planar rod on a foundation in the absence of body couple (see Figure 14). This scenario is very common in the literature [123, 124, 125, 126, 127], and it is instructive to proceed in detail and see how the buckling emerges from our morphoelastic rods framework. The rod is naturally straight, initially planar and constrained in

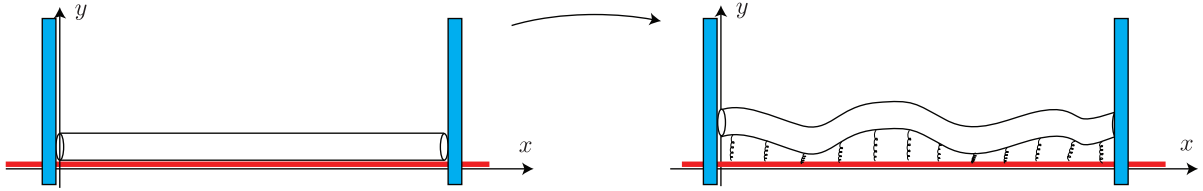


Figure 14: Setup of the buckling of a straight planar rod on a foundation. A rod is attached to a foundation and is allowed to deform only in the plane. An increase in length leads to a buckling instability.

the plane so that with respect to the reference configuration \mathcal{V} the Darboux vector is $\mathbf{u} = (0, \alpha\kappa, 0)$, where κ is the Frenet curvature. A convenient representation of the rod is obtained by assuming that it lies in the x - y plane and introducing the angle θ between the tangent vector and the x -axis. That is

$$\boldsymbol{\tau} = \mathbf{d}_3 = \cos \theta \mathbf{e}_x + \sin \theta \mathbf{e}_y, \quad (95)$$

which implies

$$\kappa = \frac{\partial \theta}{\partial s} = \alpha^{-1} \frac{\partial \theta}{\partial S} \quad (96)$$

and $\mathbf{d}_2 = \mathbf{e}_z$. By writing $\mathbf{n} = F\mathbf{e}_x + G\mathbf{e}_y$, $\mathbf{f} = f\mathbf{e}_x + g\mathbf{e}_y$, $\mathbf{r} = x\mathbf{e}_x + y\mathbf{e}_y$, we can simplify the equilibrium equations (36-37) to a system of 5 equations in the current configuration

$$\frac{\partial x}{\partial S} = \alpha \cos \theta, \quad \frac{\partial y}{\partial S} = \alpha \sin \theta, \quad (97)$$

$$\frac{\partial F}{\partial S} + f = 0, \quad \frac{\partial G}{\partial S} + g = 0, \quad (98)$$

$$EI \frac{\partial^2 \theta}{\partial S^2} + \alpha G \cos \theta - \alpha F \sin \theta = 0. \quad (99)$$

These equations are supplemented by the constitutive law for the foundation (see below) and a constitutive law for tension $F \cos \theta + G \sin \theta = EA(\alpha - 1)$ where A is the cross sectional area as before. We use this last relationship to express α in terms of F, G and θ in the equations above.

We consider the case of a clamped uniformly growing rod of initial length $L_0 = 1$ and whose end positions are fixed for all time, that is

$$x(0) = 0, \quad x(L) = 1, \quad y(L) = y(0) = y_0, \quad \theta(0) = \theta(L) = 0. \quad (100)$$

where y_0 is the distance between the rod and the rigid foundation taken to be the segment of the x -axis between 0 and 1. Different assumptions on the nature of the attachment between the rod and the foundation can be made. We consider here the case where the rod is initially glued to the axis. Therefore, a point $(S_0, 0)$ on the x -axis is attached to a point (S_0, y_0) on the rod. In the current configuration the two points are still connected elastically and are now located at $(S/\gamma, 0)$ and $(x(S), y(S))$. Therefore, the body force acting on the rod from the foundation is

$$\mathbf{f} = \frac{h(\Delta)}{\gamma\Delta} [(x - S/\gamma)\mathbf{e}_x + (y - y_0)\mathbf{e}_y] \quad (101)$$

where we have assumed that the rest length of the foundation is y_0 and $\Delta = \sqrt{(x - S/\gamma)^2 + (y - y_0)^2}$ is the distance in the current configuration between two material points connected in the initial configuration. Note the factor $1/\gamma$ which indicates that the attachment was made in the initial configuration and no subsequent remodeling takes place. The function $h(\Delta)$ is chosen such that $h(0) = 0$ and $h'(0) = -Ek < 0$.

The trivial solution is a straight compressed rod, that is

$$x^{(0)} = S/\gamma, \quad y^{(0)} = \theta^{(0)} = G^{(0)} = 0, \quad F^{(0)} = EA \frac{1-\gamma}{\gamma}. \quad (102)$$

To find the critical value of γ where a bifurcation first occurs, we expand our 5 variables in power series $x = x^{(0)} + \epsilon x^{(1)} + O(\epsilon^2)$, $y = y^{(0)} + \epsilon y^{(1)} + O(\epsilon^2)$ and, as before, linearise the system around the trivial compressed state. To first order, it is easy to show that $x^{(1)} = F^{(1)} = 0$, and we reduce the problem to a set of 3 linear equations

$$\frac{dy^{(1)}}{dS} = \frac{\theta^{(1)}}{\gamma}, \quad \frac{dG^{(1)}}{dS} = Ek \frac{y^{(1)}}{\gamma}, \quad (103)$$

$$EI \frac{d^2\theta^{(1)}}{dS^2} + EA(\gamma - 1)\theta^{(1)} + \gamma G^{(1)} = 0. \quad (104)$$

which can easily be reduced to a single fourth order differential equation for $\theta^{(1)}$

$$\frac{d^4\theta^{(1)}}{dS^4} + 2a \frac{d^2\theta^{(1)}}{dS^2} + b^2\theta^{(1)} = 0, \quad (105)$$

where

$$a = \frac{A(\gamma - 1)}{2I\gamma^2}, \quad b = \sqrt{\frac{k}{I\gamma^3}}, \quad (106)$$

and the boundary conditions (vanishing for all linearised variables) now read

$$\theta^{(1)}(0) = A(\gamma - 1) \frac{d\theta^{(1)}}{dS}(0) + I\gamma^2 \frac{d^3\theta^{(1)}}{dS^3}(0) = 0, \quad (107)$$

$$\theta^{(1)}(\gamma) = A(\gamma - 1) \frac{d\theta^{(1)}}{dS}(\gamma) + I\gamma^2 \frac{d^3\theta^{(1)}}{dS^3}(\gamma) = 0. \quad (108)$$

We now look for modes for Equation (105) of the form $\theta^{(1)} \sim e^{i\omega s}$, which leads to the 4 roots

$$\omega_1^2 = a + \sqrt{a^2 - b^2}, \quad \omega_2^2 = a - \sqrt{a^2 - b^2}. \quad (109)$$

The condition $a = b$ gives the first bifurcation condition for the existence of oscillatory modes on an infinite domain. Explicitly, it reads

$$A^2(\gamma - 1)^2 - 4Ik\gamma = 0 \quad (110)$$

which leads, for a circular cross section of radius r , to the first condition $\gamma_1 = 1 + kr(r + \sqrt{kr^2 + 4\pi})/(2\pi)$ associated with a typical mode number $n = \sqrt{a}$, that is a typical wavelength

$$\zeta = 2\pi/\omega_1 = 2\pi\gamma_1^{3/4} \left(\frac{I}{k}\right)^{1/4} = \frac{\pi^{5/4}}{\sqrt{2}} \gamma_1^{3/4} r k^{-1/4} \quad (111)$$

$$\approx r \frac{\pi^{1/4}}{\sqrt{2}} \left(\pi k^{-1/4} - \frac{\sqrt{\pi}}{4} k^{1/4} + \frac{1}{32} k^{3/4} \right) + O(k^{5/4}). \quad (112)$$

In a finite domain with clamped boundary conditions, there is a delay at the bifurcation and the value of $\gamma_2 > \gamma_1$ for which the system is unstable can be found by matching the boundary conditions. Assuming $a > b$, the non-trivial solution reads

$$\theta^{(1)} = C_1 [\cos(\omega_1 S) - \cos(\omega_2 S)] + C_2 \sin(\omega_1 S) + C_3 \sin(\omega_2 S) \quad (113)$$

with

$$C_2 = \frac{C_1 \omega_1 b (\cos(\gamma \omega_1) - \cos(\gamma \omega_2))}{(2a\omega_1 - \omega_1^3) \sin(\gamma \omega_2) + (\omega_2^3 - 2a\omega_2) \sin(\gamma \omega_1)}, \quad (114)$$

$$C_3 = \frac{C_1 \omega_2 b (\cos(\gamma \omega_2) - \cos(\gamma \omega_1))}{(2a\omega_1 - \omega_1^3) \sin(\gamma \omega_2) + (\omega_2^3 - 2a\omega_2) \sin(\gamma \omega_1)}, \quad (115)$$

with the condition

$$a \sin(\gamma \omega_1) \sin(\gamma \omega_2) + b \cos(\gamma \omega_1) \cos(\gamma \omega_2) - b = 0. \quad (116)$$

The first positive root of this equation is γ_1 but it leads to the trivial solution $\theta^{(1)} = 0$ so that the critical bifurcation value for γ is the first root $\gamma_2 > \gamma_1$. However for $r \ll L_0$, the root γ_1 provides an excellent first approximation for the critical value γ_2 . Note that this linear analysis is very close to the classical problem of a beam on a foundation [128] and indeed the force at buckling could have been predicted by a simpler theory (the main difference being that our rod is extensible). Nevertheless, we showed that this classical bifurcation can easily be obtained within the general framework of morphoelastic rods. Note also that the linear analysis presented here can also be completed by a general weakly nonlinear analysis to obtain the amplitude as a function of the load (see for instance [129, 105]).

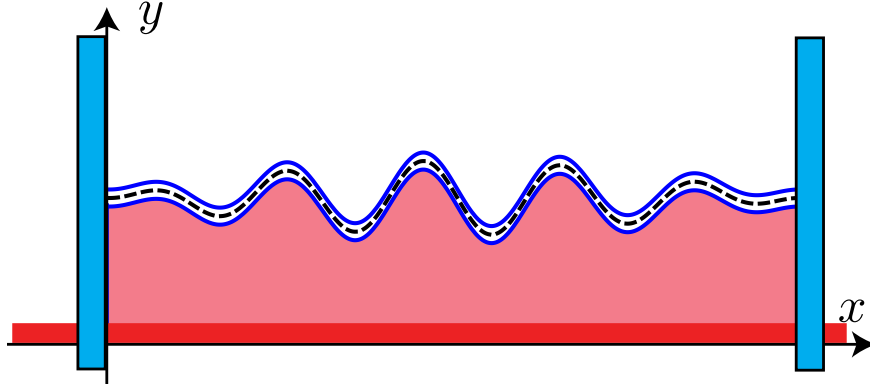


Figure 15: Buckling of a clamped growing rod on an elastic foundation. The rod is constrained to lie in the unit interval $L_0 = 1$ and is clamped at the boundary (with $y_0 = 1/2$). Here $k = 1, r = 0.02$, and $\gamma_2 = 1.19934$. The amplitude is arbitrary and chosen here to be $C_1 = -0.2$ and the centreline is indicated by a dashed line.

7.3. Spatial deformations

In the previous section, the rod was assumed to remain planar. This is a very typical assumption in models of rods on foundations. However, the question remains whether a planar deformation is a valid assumption. Here we explore this issue in the context of a rod with non-circular cross section. The setup is pictured in Figure 16. We assume an infinite, extensible, naturally straight rod that is positioned in its initial configuration parallel to the z -axis and take the foundation to be the z -axis. The cross section is assumed elliptical, with antipodal points at distances a_1 and a_2 from the centre of the ellipse, and aligned along the x and y directions, respectively, in the initial configuration. As in the previous section, we compute the critical growth at which the rod buckles to a non-straight configuration, but here we allow for a fully general 3D deformation.

The prebuckled solution consists of a straight, compressed rod. Let the initial frame correspond to the Cartesian axes, that is $\mathbf{d}_1^{(0)} = \mathbf{e}_x$, $\mathbf{d}_2^{(0)} = \mathbf{e}_y$, $\mathbf{d}_3^{(0)} = \mathbf{e}_z$. Then we can write $\mathbf{r}^{(0)} = a_1 \mathbf{d}_1^{(0)} + S \gamma^{-1} \mathbf{d}_3^{(0)}$. We

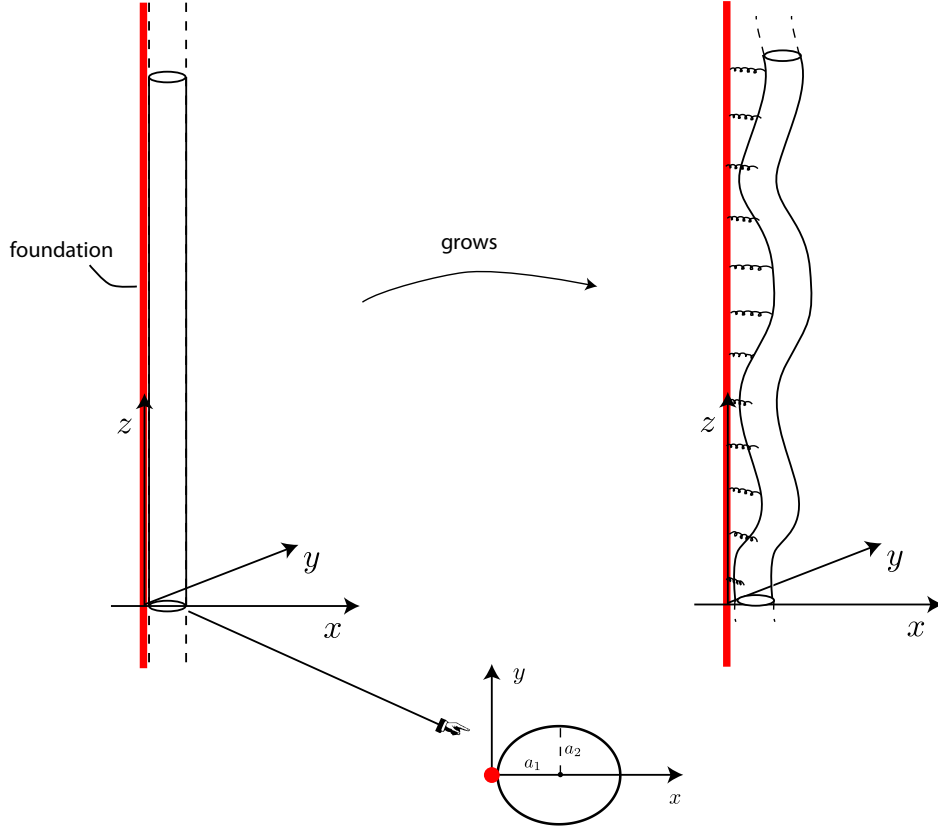


Figure 16: Setup of the buckling of a straight rod on a foundation. A rod with elliptical cross-section is attached to a foundation, the z -axis. An increase in length leads to a buckling instability.

also have $\alpha^{(0)} = 1/\gamma$, $\mathbf{n}_3^{(0)} = EA(\gamma^{-1} - 1)$, with all other quantities zero. Note that for an elliptical cross section, the constitutive equation can be written as $\mathbf{m} = B_1 \mathbf{u}_1 \mathbf{d}_1 + B_2 \mathbf{u}_2 \mathbf{d}_2 + B_3 \mathbf{u}_3 \mathbf{d}_3$, where (see [99])

$$B_1 = \frac{E\pi a_1 a_2^3}{4}, \quad B_2 = \frac{E\pi a_1^3 a_2}{4}, \quad B_3 = \frac{E\pi a_1^3 a_2^3}{2(1+\sigma)(a_1^2 + a_2^2)}, \quad (117)$$

where σ is the Poisson ratio. The body force due to the foundation is $\mathbf{f} = k(\boldsymbol{\rho} - \mathbf{r}_A)$, with the attachment point $\mathbf{r}_A = \mathbf{r} - a_1 \mathbf{d}_1$. Twist is permitted in the buckling, and the body couple is given by Equation (52). The body force and couple are zero in the prebuckled solution, and have components in the perturbed solution given by

$$\begin{aligned} f_1^{(1)} &= -kr_1^{(1)}, \quad f_2^{(1)} = -k(r_2^{(1)} - a_1 c_3), \quad f_3^{(1)} = -k(r_3^{(1)} + a_1 c_2), \\ l_2^{(1)} &= a_1 f_3^{(1)}, \quad l_3^{(1)} = -a_1 f_2^{(1)}. \end{aligned} \quad (118)$$

The system of equations for the first order components of the buckled rod decouples into 5 equations for $\mu_1 := [r_1^{(1)}, r_3^{(1)}, c_2, n_1^{(1)}, n_3^{(1)}]^T$ and 4 equations for $\mu_2 := [r_2^{(1)}, c_1, c_3, n_2^{(1)}]^T$. Thus the buckling will tend to occur in one set of variables or the other. Denote a bifurcation in the first and second sets respectively as Type I and II. To form the determinant condition for buckling, we allow different wavelengths for each type, that is we assume a form $\mu_j = \xi e^{in_j S\pi/\gamma} + \bar{\xi} e^{-in_j S\pi/\gamma}$, $j = 1, 2$. A critical growth can be determined for each solution type; that is, we can find both γ_I^* and γ_{II}^* , and the buckling point and type is determined by the smaller of the two.

No foundation.. In the absence of a foundation, the critical growth takes the simple form

$$\gamma_I^*(n_1) = \frac{B_2 \pi^2 n_1^2}{k} + 1, \quad \gamma_{II}^*(n_2) = \frac{B_1 \pi^2 n_2^2}{k} + 1. \quad (119)$$

Note that for a circular cross section ($a_1 = a_2$), $B_1 = B_2$, and thus the critical growths are equivalent for each buckling direction. If $a_1 > a_2$, then $B_1 < B_2$, and so for a given mode $n_1 = n_2 = n$, it follows that $\gamma_{II}^* < \gamma_I^*$, while $a_1 < a_2 \Rightarrow B_2 < B_1 \Rightarrow \gamma_I^* < \gamma_{II}^*$. This reflects the intuitive fact that a rod will tend to buckle in the direction where the cross section is thinner, i.e. it will buckle about the direction aligned with the major axis of the ellipse.

Effect of foundation.. For a circular cross section, with $a_1 = a_2 = a$, we find that for all material parameters and foundation stiffnesses, $\gamma_{II}^* < \gamma_I^*$. That is, *a rod with circular cross section will always buckle as a Type II solution*. Recall that the rod is situated such that it passes through the x -axis in the natural configuration, and that Type II solutions consist of a deformation in the y -direction. Thus the rod becomes unstable first in the direction orthogonal to the direction in which the “springs” are aligned. This is interesting in the context of the beam on a foundation analysis, in which the deformation is assumed to occur in the x - z plane of our setup. Indeed, this was the case in the previous section. Here, we have shown that in fact for a circular cross section, buckling will initially occur in the orthogonal, y - z plane.

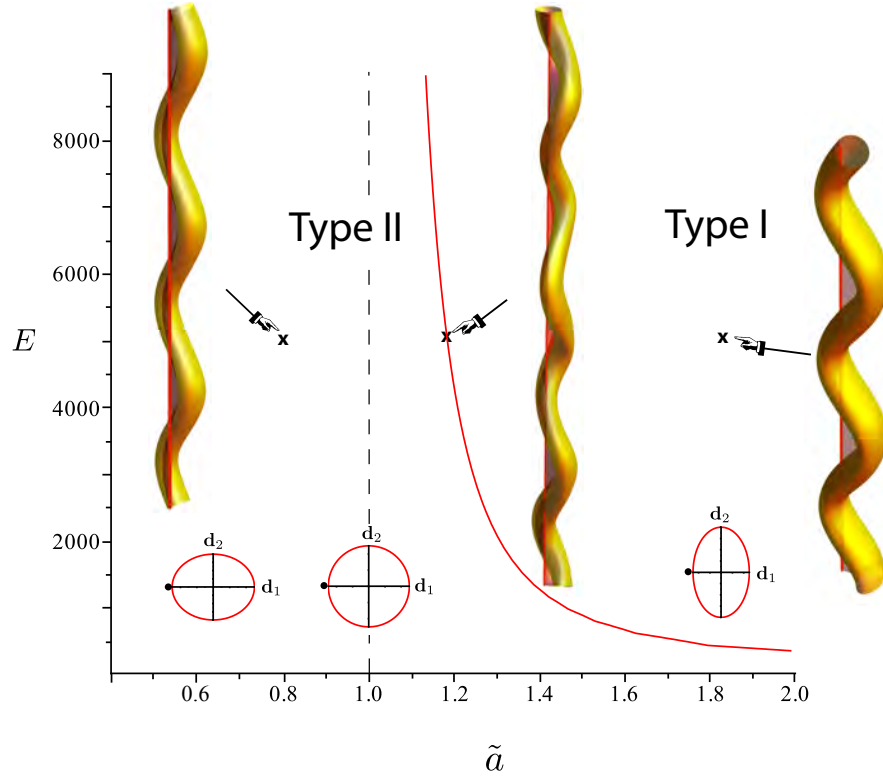


Figure 17: Phase diagram of the buckling of a rod on a straight foundation. The curve divides the E - \tilde{a} plane by type and direction of the initial instability. On the curve, both types are triggered, and the instability is of mixed type. Other parameters: $a_1 = 0.05$, $\sigma = 0.3$, $k_f = 100$.

For non-circular cross sections, however, Type I bifurcations can be triggered. Figure 17 shows a phase diagram in the E - \tilde{a} plane, where $\tilde{a} := a_2/a_1$. To the left of the curve, $\gamma_{II}^* < \gamma_I^*$, and the buckling is Type II. Observe that the entire line $\tilde{a} = 1$ is in this region. To the right of the curve, $\gamma_I^* < \gamma_{II}^*$, and the buckling is Type I. We see that as the Young's modulus E decreases, the buckling disparity is enhanced, so that the elliptical cross section must be more eccentric with major axis in the d_2 direction (i.e. the y -direction of the pre-buckled rod). Also of interest is that *on the curve*, $\gamma_I^* = \gamma_{II}^*$, and thus the form of the buckled solution is of mixed type. These solutions can have an unusual form, since the two combined types will typically occur at different wavenumbers, that is $n_1 \neq n_2$ (also, since we consider an infinite rod, there is no requirement that the n_i are integers). An example is given in Figure 17 (but again, a weakly nonlinear analysis would be needed to determine the amplitudes of the buckling types).

8. Conclusions

We have proposed a systematic formulation of growing elastic rods based on the Kirchhoff equations. This formulation is generic in the sense that it can be easily adapted to many different problems involving elastic filamentary structures undergoing growth and large deformations. Like most mechanical theories, the theory developed in this paper relies on three different components: kinematics, mechanics, and constitutive laws.

First, the kinematics is characterised by the introduction of three different configurations. The initial configuration before growth, an unstressed reference configuration after growth, and a current configuration depending on the loads and boundary conditions. The passage from the initial to the reference configurations is mostly given by a growth stretch (γ) characterising the elongation of the rod purely due to growth. That is, it contains information on the axial extension due to growth in the unloaded filaments.

Second, the mechanics of a growing rod follows directly from the basic mechanical principles of a Kirchhoff elastic rod and is completely contained in the usual balance of forces and moments. For simplicity, we advocate to use the material arc length in the reference configuration as the main independent variable as it is conceptually easier to define material properties in that particular configuration.

Finally, the mechanics and kinematics must be supplemented by constitutive laws. For many problems of interest in growing rods, there are three different type of laws. First, the constitutive law for the material properties of the rod (relating stresses to strains). Again, these are the usual laws in a classical theory of elastic rods and depending on the level of details required, one may use various forms of energy density (quadratic, isotropic, inextensible, unshearable,...). Second is the interaction of the rod with the external world. Here, the focus was on attachment to a rigid foundation, which requires a foundation law; that is, the constitutive equations that describe the attachment. These laws contain the overall response of the foundation to deformation and include details about the nature of the elastic material in the foundation and the way it is connected to the rod. Since forces act in the current configuration, the constitutive laws for the foundations are best formulated in that particular configuration. Third is the evolution law for the growth parameter, which relates the anelastic part of the deformation to external fields (position, stress, strain,...).

Using our formulation for growing rods, we have demonstrated that instabilities of different natural configurations (free or on a foundation) can emerge through the growth evolution. In particular, we have considered a series of examples involving the buckling of rings and straight rods, and have explicitly shown the effect of different growth laws, foundation attachments, and material parameters.

The foundation that we used was assumed to be a connection between an elastic rod and a rigid curve or surface. Alternatively, an elastic rod can be connected to other elastic rods through either a rigid constraint or through a foundation. The problem is then to capture the equilibrium shape of the connected rods when they are allowed to grow (or twist) at different rates. We will explore possible equilibrium configurations of multiple connected rods in the second installment of this series ([100]).

Acknowledgments: This publication is based on work supported by Award No. KUK-C1-013-04, made by King Abdullah University of Science and Technology (KAUST), and based in part upon work supported by the National Science Foundation under grants DMS-0907773 (AG). AG is a Wolfson Royal Society Merit Holder and is supported by a Reintegration Grant under EC Framework VII. TL is a Marie Curie Fellow under EC Framework VII and also gratefully acknowledges support from the “Fondation Wiener-Anspach”.

References

- [1] A. Goriely and M. Tabor. The nonlinear dynamics of filaments. *Nonlinear Dynam.*, 21(1):101–133, 2000.
- [2] E. E. Zajac. Stability of two planar loop elasticas. *ASME J. Applied Mech.*, March:136–142, 1962.
- [3] M. D. Barkley and B. H. Zimm. Theory of twisting and bending of chain macromolecules; analysis of the fluorescence depolarization of DNA. *J. Chem. Phys.*, 70, 1979.
- [4] H. C. Spruit. Motion of magnetic flux tubes in the solar convection zone and chromosphere. *Astron. Astrophys.*, 98:155, 1981.
- [5] C. J. Benham. An elastic model of the large structure of duplex DNA. *Biopolymers*, 18:609–623, 1979.
- [6] C. J. Benham. Geometry and mechanics of DNA superhelicity. *Biopolymers*, 22:2477–2495, 1983.
- [7] J. P. Keener. Knotted vortex filament in an ideal fluid. *J. Fluid Mech.*, 211, 1990.
- [8] S. Da Silva and A. R. Chouduri. A theoretical model for tilts of bipolar magnetic regions. *Astron. Astrophys.*, 272:621, 1993.
- [9] R. S. Manning, J. H. Maddocks, and J. D. Kahn. A continuum rod model of sequence-dependent DNA structure. *J. Chem. Phys.*, 105:5626–5646, 1996.
- [10] J. M. T. Thompson, G. H. M. van der Heijden, and S. Neukirch. Supercoiling of DNA plasmids: mechanics of the generalized ply. *Proc. R. Soc. A*, 458:959–985, 2002.
- [11] N. H. Mendelson. Helical *Bacillus subtilis* macrofibers: morphogenesis of a bacterial multicellular macroorganism. *Proc. Natl. Acad. Sci. USA*, 75, 1978.
- [12] I. Klapper and M. Tabor. Dynamics of twist and writhe and the modeling of bacterial fibers. In J. Mesirov, K. Schuitens, and De Witt Summers, editors, *Mathematical Approaches to Biomolecular Structure and Dynamics*. Springer, 1996.
- [13] A. Goriely, M. Robertson-Tessi, M. Tabor, and R. Vandiver. Elastic growth models. In R. Mondaini and P. M. Pardalos, editors, *Mathematical Modelling of Biosystems*, volume 12 of *Applied Optimization*. Springer, 2008.
- [14] D. I. Gray, G. W. Gooday, and J. I. Prosser. Apical hyphal extension in *streptomyces coelicolor* A3(2). *J. Gen. Microbiol*, 136:1077, 1990.
- [15] J. A. Shapiro and M. Dworkin, editors. *Mycelial life of Streptomyces coelicolor A3(2) and its relatives*, volume Bacteria as multicellular organisms. Oxford University Press, Oxford, 1997.
- [16] A. Goriely and M. Tabor. Biomechanical models of hyphal growth in actinomycetes. *J. Theor. Biol.*, 222:211–218, 2003.
- [17] A. Goriely and M. Tabor. Self-similar tip growth in filamentary organisms. *Phys. Rev. Lett.*, 90(10):108101, 2003.
- [18] NF Robertson. The growth process in fungi. *Annu. Rev. Phytopathol.*, 6(1):115–136, 1968.
- [19] K. Bergman, P.V. Burke, E. Cerdá-Olmedo, C.N. David, M. Delbrück, KW Foster, EW Goodell, M. Heisenberg, G. Meissner, M. Zalokar, et al. Phycomyces. *Bacteriol. Rev.*, 33(1):99, 1969.
- [20] A. L. Koch. The problem of hyphal growth in streptomycetes and fungi. *J. Theor. Biol.*, 171(2):137–150, 1994.
- [21] A. Goriely and M. Tabor. Spontaneous Rotational Inversion in Phycomyces. *Phys. Rev. Lett.*, 106(13):138103, 2011.
- [22] J. Dumais, S. R. Long, and S. L. Shaw. The Mechanics of Surface Expansion Anisotropy in *Medicago truncatula* Root Hairs. *Plant Physiol.*, 136:3266–3275, 2004.

- [23] P.A. Roelofsen and AL Houwink. Architecture and growth of the primary cell wall in some plant hairs and in the phycomyces sporangiophore. *Acta. Bot. Neerl.*, 2:218–225, 1953.
- [24] S. L. Shaw, J. Dumais, and S. R. Long. Cell surface expansion in polarly growing root hairs of *medicago truncatula*. *Plant Physiol.*, 124:959–969, 2000.
- [25] W. K. Silk and A. Haidar. Growth of the stem of *Pharbitis nil*: Analysis of longitudinal and radial components. *Physiol. Veg.*, 24, 1986.
- [26] W. K. Silk. On the curving and twining of stems. *Environ. Exper. Bot.*, 29:95–109, 1989.
- [27] C. R. Steele. Shell stability related to pattern formation in plants. *J. Appl. Mech.*, 67, 2000.
- [28] A. Goriely and S. Neukirch. Mechanics of climbing and attachment in twining plants. *Phys. Rev. Lett.*, 97(18):184302, 2006.
- [29] B. Moulia, C. Coutand, and C. Lenne. Posture control and skeletal mechanical acclimation in terrestrial plants: implications for mechanical modeling of plant architecture. *Am. J. Bot.*, 93(10):1477, 2006.
- [30] T. Speck and I. Burgert. Plant stems: Functional design and mechanics. *Annu. Rev. Mater. Res.*, 41:169–193, 2011.
- [31] A. Chavarría-Krauser, W. Jäger, and U. Schurr. Primary root growth: a biophysical model of auxin-related control. *Funct. Plant Biol.*, 32:849–862, 2005.
- [32] R.O. Erickson and K.B. Sax. Elemental growth rate of the primary root of *Zea mays*. *Proc. Am. Philos. Soc.*, 100(5):487–498, 1956.
- [33] J.L. Mullen, E. Turk, K. Johnson, C. Wolverton, H. Ishikawa, C. Simmons, D. Soll, and M.L. Evans. Root-growth behavior of the *Arabidopsis* mutant *rgl1*. Roles of gravitropism and circumnutation in the waving/coiling phenomenon. *Plant Physiol.*, 118(4):1139, 1998.
- [34] K. Okada and Y. Shimura. Reversible root tip rotation in *Arabidopsis* seedlings induced by obstacle-touching stimulus. *Science*, 250(4978):274, 1990.
- [35] H. Buschmann, M. Hauptmann, D. Niessing, C.W. Lloyd, and A.R. Schäffner. Helical growth of the *Arabidopsis* mutant *tortifolia2* does not depend on cell division patterns but involves handed twisting of isolated cells. *Plant Cell*, 21(7):2090, 2009.
- [36] J. B. Keller. Tendril shape and lichen growth. *Lecture on Mathematics in the Life Science*, 30, 1980.
- [37] A. Goriely and M. Tabor. Spontaneous helix-hand reversal and tendril perversion in climbing plants. *Phys. Rev. Lett.*, 80:1564–1567, 1998.
- [38] T. McMillen and A. Goriely. Tendril perversion in intrinsically curved rods. *J. Nonlinear Sci.*, 12(3):241–281, 2002.
- [39] R. E. Goldstein and A. Goriely. Dynamic buckling of morphoelastic filaments. *Phys. Rev. E*, 74:010901, 2006.
- [40] P. W. Barlow, P. Brain, and J. S. Adam. Differential growth and plant tropism: a study assisted by computer simulation. *Environmental Exp. Bot.*, 29, 1989.
- [41] T J Dennerll, P Lamoureux, R E Buxbaum, and S R Heidemann. The cytomchanics of axonal elongation and retraction. *J. Cell Biol.*, 109(6 Pt 1):3073–83, Dec 1989.
- [42] P Lamoureux, R E Buxbaum, and S R Heidemann. Direct evidence that growth cones pull. *Nature*, 340(6229):159–62, Jul 1989.
- [43] S Chada, P Lamoureux, R E Buxbaum, and S R Heidemann. Cytomechanics of neurite outgrowth from chick brain neurons. *J. Cell Sci.*, 110 (Pt 10):1179–86, May 1997.

- [44] P Lamoureux, J Zheng, R E Buxbaum, and S R Heidemann. A cytomachanical investigation of neurite growth on different culture surfaces. *J. Cell Biol.*, 118(3):655–61, Aug 1992.
- [45] Phillip Lamoureux, Gordon Ruthel, Robert E Buxbaum, and Steven R Heidemann. Mechanical tension can specify axonal fate in hippocampal neurons. *J. Cell Biol.*, 159(3):499–508, Nov 2002.
- [46] A. Goriely. Knotted umbilical cords. In J. A. Calvo, A. Stasiak, and E. Rawdon, editors, *Physical and Numerical Models in Knot Theory Including Their Application to the Life Sciences*, pages 109–126. World Scientific, Singapore, 2004.
- [47] A. E. Miller, M. C. Jones, and D. W. Smith. Tension: the basis of umbilical cord growth. *J. Pediatr.*, 101:844, 1982.
- [48] IJ Rao, JD Humphrey, and KR Rajagopal. Biological growth and remodeling: A uniaxial example with possible application to tendons and ligaments. *Comput. Model. Eng. Sci.*, 4(3/4):439–456, 2003.
- [49] P. W. Alford, J. D. Humphrey, and L. A. Taber. Growth and remodeling in a thick-walled artery model: effects of spatial variations in wall constituents. *Biomech. Model Mechanobiol.*, 7:245–262, 2007.
- [50] L. A. Taber and J. D. Humphrey. Stress-modulated growth, residual stress, and vascular heterogeneity. *J. Biomech. Eng.*, 123:528–535, 2001.
- [51] A. Goriely and R. Vandiver. On the mechanical stability of growing arteries. *IMA J. Appl. Math.*, Accepted:122, 2010.
- [52] V. M. Entov. Mechanical model of scoliosis. *Mech. Solids*, 18, 1983.
- [53] R. Skalak. Growth as a finite displacement field. In D. E. Carlson and R. T. Shield, editors, *Proceedings of the IUTAM Symposium on Finite Elasticity*. Martinus Nijhoff, The Hague, 1981.
- [54] R. Skalak, G. Dasgupta, M. Moss, E. Otten, P. Dullemeijer, and H. Vilmann. Analytical description of growth. *J. Theor. Biol.*, 94(555-577), 1982.
- [55] E. K. Rodriguez, A. Hoger, and A. McCulloch. Stress-dependent finite growth in soft elastic tissue. *J. Biomech.*, 27:455–467, 1994.
- [56] A. A. Stein. The deformation of a rod of growing biological material under longitudinal compression. *J. Appl. Math. Mech.*, 59, 1995.
- [57] A. Rachev. Theoretical study of the effect of stress-dependent remodeling on arterial geometry under hypertensive conditions. *J. Biomech.*, 30:819–827, 1997.
- [58] D. Ambrosi, GA Ateshian, EM Arruda, SC Cowin, J. Dumais, A. Goriely, GA Holzapfel, JD Humphrey, R. Kemkemer, E. Kuhl, et al. Perspectives on biological growth and remodeling. *J. Mech. Phys. Solids*, 2010.
- [59] A. L. Koch. The problem of hyphal growth in streptomycetes and fungi. In A. L. Koch, editor, *Bacterial Growth and Form*. Chapman & Hall, New York, 1995.
- [60] H. R. Duhamel du Monceau. La physique des arbres (The physics of trees). *L. Guérin et L.-F. Delatour, Paris, France*, 1758.
- [61] Phillip Lamoureux, Steven R Heidemann, Nathan R Martzke, and Kyle E Miller. Growth and elongation within and along the axon. *Dev. Neurobiol.*, 70(3):135–49, Feb 2010.
- [62] M. Fournier, PA Bordonne, D. Guitard, and T. Okuyama. Growth stress patterns in tree stems. *Wood Sci. Technol.*, 24(2):131–142, 1990.
- [63] M. Fournier, B. Chanson, B. Thibaut, and D. Guitard. Mechanics of standing trees: modelling a growing structure submitted to continuous and fluctuating loads. 2. tridimensional analysis of maturation stresses. case of standard hardwood [cambial growth]. In *Annales des Sciences Forestieres*, volume 48, 1991.

- [64] M. Fournier, A. Stokes, C. Coutand, T. Fourcaud, B. Moulia, et al. Tree biomechanics and growth strategies in the context of forest functional ecology. *Ecology and biomechanics: a mechanical approach to the ecology of animals and plants*. Boca Raton, Taylor & Francis Group, pages 1–33, 2006.
- [65] Z.S. Jackson, A.I. Gotlieb, and B.L. Langille. Wall Tissue Remodeling Regulates Longitudinal Tension in Arteries. *Circ. Res.*, 90(8):918–925, 2002.
- [66] W. S. Peters and A. D. Tomos. The history of tissue tension. *Ann. Bot-London*, 77(6):657–65, 1996.
- [67] R. Vandiver and A. Goriely. Tissue tension and axial growth of cylindrical structures in plants and elastic tissues. *Europhys. Lett.*, 84(58004), 2008.
- [68] S. P. Timoshenko. Analysis of bi-metal thermostats. *J. Opt. Soc. Am.*, 11(3):233–255, 1925.
- [69] D. Burgreen and P.J. Manitt. Thermal buckling of a bimetallic beam. *J. Eng. Mech. Div.-ASCE*, 95:421–32, 1969.
- [70] D. Burgreen and D. Regal. Higher mode buckling of bimetallic beam. *J. Eng. Mech. Div.-ASCE*, 97(4):1045–1056, 1971.
- [71] Z. Hejnowicz. Gravitropism in herbs and trees: a major role for the redistribution of tissue and growth stresses. *Planta*, 203(5):136–146, 1997.
- [72] P. Galland. Tropisms of Avena coleoptiles: sine law for gravitropism, exponential law for photogravitropic equilibrium. *Planta*, 215(5):779–784, 2002.
- [73] B. Moulia and M. Fournier. The power and control of gravitropic movements in plants: a biomechanical and systems biology view. *J. Exp. Bot.*, 60(2):461, 2009.
- [74] P. R. Bell. Twining of the hop (*Humulus lupulus* L.). *Nature*, 181:1009–1010, 1958.
- [75] W. K. Silk, N. M. Holbrook, and C. Jessup. The forceful nature of twining vines. *Plant biomechanics*, pages 638–646, 2000.
- [76] A. Goriely, G. Karolyi, and M. Tabor. Growth induced curve dynamics for filamentary micro-organisms. *J. Math. Biol.*, 51(3):355–366, 2005.
- [77] D.E. Moulton and A. Goriely. Surface growth kinematics via local curve evolution. *Preprint*, 2012.
- [78] B. D. Coleman, E. H. Dill, M. Lembo, Z. Lu, and I. Tobias. On the dynamics of rods in the theory of Kirchhoff and Clebsch. *Arch. Rational Mech. Anal.*, 121:339–359, 1993.
- [79] D.J. Dichmann, Y. Li, and J.H. Maddocks. Hamiltonian formulations and symmetries in rod mechanics. *IMA Vol. Math. Appl.*, 82:71–114, 1996.
- [80] S. S. Antman. *Nonlinear problems of elasticity*. Springer New York, 2005.
- [81] P. Villaggio. *Mathematical models for elastic structures*. Cambridge University Press, Cambridge, 1997.
- [82] N.A. Faruk Senan, O.M. O’Reilly, and T.N. Treslerras. Modeling the growth and branching of plants: A simple rod-based model. *J. Mech. Phys. Solids*, 56(10):3021–3036, 2008.
- [83] O. M. O’Reilly and T. N. Treslerras. On the Static Equilibria of Branched Elastic Rods. *Preprint submitted to Int. J. Eng. Sci.*, 2010.
- [84] OM O’Reilly and TN Treslerras. On the evolution of intrinsic curvature in rod-based models of growth in long slender plant stems. *Int. J. Solids Struct.*, 2010.
- [85] T. Guillon, Y. Dumont, and T. Fourcaud. A new mathematical framework for modelling the biomechanics of growing trees with rod theory. *Math. Comput. Model.*, 2011.
- [86] Y. Renardy, A. V. Coward, D. Papageorgiou, and S. M. Sun, editors. *The nonlocal dynamics of stretching, buckling filaments*, volume Advances in multi-fluid flows. SIAM, Philadelphia, 1996.

- [87] C.W. Wolgemuth, R.E. Goldstein, and T.R. Powers. Dynamic supercoiling bifurcations of growing elastic filaments. *Physica D*, 190(3):266–289, 2004.
- [88] AE Green and PM Naghdi. Non-isothermal theory of rods, plates and shells. *Int. J. Solids Struct.*, 6(2):209–244, 1970.
- [89] AE Green and PM Naghdi. On thermal effects in the theory of rods. *Int. J. Solids Struct.*, 15(11):829–853, 1979.
- [90] J. Cisternas and P. Holmes. Buckling of extensible thermoelastic rods. *Math. Comput. Modelling*, 36(3):233–243, 2002.
- [91] A. Yavari. A geometric theory of growth mechanics. *J. Nonlinear Sci.*, 20:781–830, 2010.
- [92] S. S. Antman. *Nonlinear problems of elasticity*. Springer Verlag, New York, 1995.
- [93] JH Maddocks. Bifurcation theory, symmetry breaking and homogenization in continuum mechanics descriptions of dna. *A Celebration of Mathematical Modeling: The Joseph B. Keller Anniversary Volume*, pages 113–136, 2004.
- [94] G. L. Jr. Lamb. Solitons on moving space curves. *J. Math. Phys.*, 18, 1977.
- [95] M. Lakshmanan. Rigid body motions, space curves, prolongation structures, fiber bundles, and solitons. *J. Math. Phys.*, 20, 1979.
- [96] R. E. Goldstein and D. M. Petrich. The Korteweg-de Vries hierarchy as dynamics of closed curves in the plane. *Phys. Rev. Lett.*, 67, 1991.
- [97] K. Nakayama, H. Segur, and M. Wadati. Integrability and the motion of curves. *Phys. Rev. Lett.*, 69, 1992.
- [98] A. Doliwa and P. M. Santini. The integrable dynamics of discrete and continuous curves. *Preprint*, 1995.
- [99] A. Goriely, M. Nizette, and M. Tabor. On the dynamics of elastic strips. *J. Nonlinear Sci.*, 11:3–45, 2001.
- [100] Th. Lessines, D.E. Moulton, and A. Goriely. Morphoelastic rods. Part II: A theory for two growing rods in interaction. *Preprint*, 2012.
- [101] M. Ben Amar and A. Goriely. Growth and instability in elastic tissues. *J. Mech. Phys. Solids*, 53:2284–2319, 2005.
- [102] A. Goriely and D.E. Moulton. Morphoelasticity - a theory of elastic growth. In Oxford University Press, editor, *New Trends in the Physics and Mechanics of Biological Systems*, 2010.
- [103] A. Goriely, M. Nizette, and M. Tabor. On the dynamics of elastic strips. *J. Nonlinear Sci.*, 11(1):3–45, 2001.
- [104] A. Goriely and M. Tabor. Nonlinear dynamics of filaments I: Dynamical instabilities. *Phys. D*, 105:20–44, 1997.
- [105] A. Goriely and M. Tabor. Nonlinear dynamics of filaments II: Nonlinear analysis. *Phys. D*, 105:45–61, 1997.
- [106] A. Goriely. Twisted elastic rings and the rediscoveries of Michell’s instability. *J. Elasticity*, 84(3):281–299, 2006.
- [107] J. H. Michell. On the stability of a bent and twisted wire. *Messenger of Math.*, 11, 1889.
- [108] I. Tobias, B. D. Coleman, and M. Lembo. A class of exact dynamical solutions in the elastic rod model of DNA with implications for the theory of fluctuations in the torsional motion of plasmids. *J. Chem. Phys.*, 105:2517–2526, 1996.

- [109] I. Tobias and W. K. Olson. The effect of intrinsic curvature on supercoiling—Predictions of elasticity theory. *Biopolymers*, 33:639–646, 1993.
- [110] Z. Haijun and Zhong-can O.-Y. Spontaneous curvature-induced dynamical instability of Kirchhoff filaments: Application to DNA kink deformations. *J. Chem. Phys.*, 110, 1999.
- [111] P. Shipman and A. Goriely. On the dynamics of helical strips. *Phys. Rev. E*, 61, 2000.
- [112] R. S. Manning and K. A. Hoffman. Stability of n -covered circles for elastic rods with constant planar intrinsic curvature. *J. Elasticity*, 62, 2001.
- [113] W. Han, S. M. Lindsay, M. Dlakic, and R. E. Harrington. Kinked DNA. *Nature*, 386, 1997.
- [114] H. Qian and J. H. White. Terminal twist induced continuous writhe of a circular rod with intrinsic curvature. *J. Biomol. Struct. Dyn.*, 16, 1998.
- [115] S. Panyukov and Y. Rabin. Fluctuating elastic rings: statics and dynamics. *Phys. Rev. E.*, 64:#0011909, 2001.
- [116] S. Neukirch, J. Frelat, A. Goriely, and C. Maurini. Vibrations of post-buckled rods: The singular inextensible limit. *J. Sound and Vibration*, 331(3):704–720, 2012.
- [117] R.S. Manning, K.A. Rogers, and J.H. Maddocks. Isoperimetric conjugate points with application to the stability of dna minicircles. *Proc. R. Soc. Lond. Ser. A Math. Phys. Eng. Sci.*, 454(1980):3047, 1998.
- [118] S.R. Heidemann, P. Lamoureux, and R.E. Buxbaum. Cytomechanics of axonal development. *Cell Biochem. Biophys.*, 27(3):135–155, 1997.
- [119] B.J. Pfister, A. Iwata, D.F. Meaney, and D.H. Smith. Extreme stretch growth of integrated axons. *J. Neurosci.*, 24(36):7978, 2004.
- [120] D. Bray. Axonal growth in response to experimentally applied mechanical tension. *Dev. Biol.*, 102(2):379, 1984.
- [121] J. Zheng, P. Lamoureux, V. Santiago, T. Dennerll, R. E. Buxbaum, and S. R. Heidemann. Tensile regulation of axonal elongation and initiation. *J. Neurosci.*, 11(4):1117, 1991.
- [122] M. O’Toole, P. Lamoureux, and K.E. Miller. A Physical Model of Axonal Elongation: Force, Viscosity, and Adhesions Govern the Mode of Outgrowth. *Biophys. J.*, 94(7):2610–2620, 2008.
- [123] MA Biot. Bending of an infinite beam on an elastic foundation. *Zeitschrift für Angewandte Mathematik und Mechanik*, 2(3):165–184, 1922.
- [124] C.M. Edwards and S.J. Chapman. Biomechanical modelling of colorectal crypt budding and fission. *Bulletin of mathematical biology*, 69(6):1927–1942, 2007.
- [125] M. Eisenberger and J. Clastornik. Vibrations and buckling of a beam on a variable winkler elastic foundation. *Journal of sound and vibration*, 115(2):233–241, 1987.
- [126] L.D. Landau and E.M. Lifshitz. *Theory of elasticity*. Pergamon Press, 1986.
- [127] MK Wadee, G.W. Hunt, and AIM Whiting. Asymptotic and rayleigh–ritz routes to localized buckling solutions in an elastic instability problem. *Proceedings of the Royal Society of London. Series A: Mathematical, Physical and Engineering Sciences*, 453(1965):2085–2107, 1997.
- [128] W.T. Koiter and AMA Van Der Heijden. *WT Koiter’s elastic stability of solids and structures*. Cambridge Univ Press, 2009.
- [129] C. G. Lange and A. C. Newell. The post-buckling problem for thin elastic shells. *SIAM J. Appl. Math.*, 21, 1971.

A. How body couples are generated

Body couples are notoriously complicated and it is often the practice to neglect them. However, when rods are attached to a support, the support exerts a force on the rod and since this force acts on the surface of the rod and not directly on the centreline it creates a system of force and couple. The following is a simple example that illustrates how body couples are generated by these interactions. Here, we neglect growth and deformation of the central axis. We consider a naturally straight rod of circular cross section and unit length clamped between two plates a distance one apart. The mid point of the rod is twisted and then attached to a rigid foundation. That is, the rod is attached via a single “spring” at its midpoint. In this setup, the unstressed shape is untwisted, but untwisting is opposed by the spring. The setup is pictured in Figure 18, which gives a schematic of the mid point cross-section. We assume that the rod can twist while

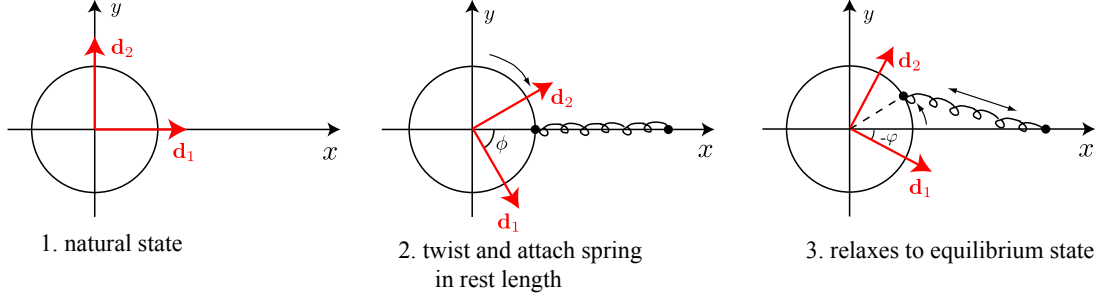


Figure 18:

its axis is constrained to remain straight. Then the centreline is determined to be along the z -axis so that $\mathbf{r}(s) = [0, 0, s]$, $0 < s < 1$. We position the foundation at the point $[L + a, 0, 1/2]$, where L is the rest length of the spring and a is the radius of the rod's cross section. The vectors \mathbf{d}_1 and \mathbf{d}_2 are oriented to align with the x and y axes, respectively, in the untwisted state. Following Figure 4, let ϕ denote the angle between the attachment point \mathbf{r}_A and the \mathbf{d}_1 axis, i.e. ϕ is the given angle of twist when the spring is in its rest length. Note the relationships

$$\mathbf{d}_1 = \cos \varphi \hat{\mathbf{x}} + \sin \varphi \hat{\mathbf{y}}, \quad \mathbf{d}_2 = -\sin \varphi \hat{\mathbf{x}} + \cos \varphi \hat{\mathbf{y}} \quad (120)$$

where φ is the register angle as described in Section 2.1.1. The attachment point is thus given by

$$\mathbf{r}_A = [a(\cos \phi \cos \varphi - \sin \phi \sin \varphi), a(\cos \phi \sin \varphi + \sin \phi \cos \varphi), 1/2]. \quad (121)$$

The attachment force \mathbf{f} is given by Equation (51) using $\rho(\mathcal{A}) = [L + a, 0, 1/2]$. Note \mathbf{f} is of the form

$$\mathbf{f} = f_x(\varphi(s); \phi) \delta(s - 1/2) \hat{\mathbf{x}} + f_y(\varphi(s); \phi) \delta(s - 1/2) \hat{\mathbf{y}}, \quad (122)$$

where $\delta(s)$ is the Dirac delta function. Since $\mathbf{r} - \mathbf{r}_A$ has only \hat{x} and \hat{y} components, the body couple, given by (52), is of the form

$$\mathbf{l} = h(\varphi(s); \phi) \delta(s - 1/2) \hat{\mathbf{z}}. \quad (123)$$

The twisting moment is $\mathbf{m}_3 = \mu J \mathbf{u}_3 = \mu J \varphi'(s)$, and thus the $\mathbf{d}_3 = \hat{\mathbf{z}}$ component of the moment balance reads

$$\mu J \varphi'' + h \delta(s - 1/2) = 0. \quad (124)$$

B. Computation of the Fourier coefficients for the growing ring

Here, we give the details for the computation of the approximate solutions for the growing ring based on its Fourier expansion. We recall that for the growing ring we have

$$\begin{aligned} \frac{1}{\gamma} \frac{du_1^*}{dS^*} &= (1 - \Gamma) u_2^* u_3^* - u_3^*, \\ \frac{1}{\gamma} \frac{du_2^*}{dS^*} &= -(1 - \Gamma) u_1^* u_3^*, \\ \frac{\Gamma}{\gamma} \frac{du_3^*}{dS^*} &= u_1^*, \end{aligned} \quad (125)$$

where $S = \gamma S^*/\hat{u}_2$, $u_i = \hat{u}_2 u_i^*$ and γ is as before the growth parameter.

The main idea is to express the three variables in (76) in terms of Fourier series, that is

$$u_n^* = \sum_{k=-\infty}^{\infty} U_n(k) e^{ikS^*} \quad (126)$$

where

$$U_n(k) = \frac{1}{2\pi} \int_0^{2\pi} e^{-ikS^*} u_n^*(S^*) dS^*, \quad U_n(k) = U_n^\dagger(-k) \quad (127)$$

and $(\)^\dagger$ indicates complex conjugation. Then, in terms of $U_n(k)$, the system (125) becomes

$$\forall k : \quad \frac{ik}{\gamma} U_1(k) = (1 - \Gamma) \sum_{p+q=k} U_2(p) U_3(q) - U_3(k), \quad (128)$$

$$\forall k : \quad \frac{ik}{\gamma} U_2(k) = -(1 - \Gamma) \sum_{p+q=k} U_1(p) U_3(q), \quad (129)$$

$$\forall k : \quad \frac{ik\Gamma}{\gamma} U_3(k) = U_1(k). \quad (130)$$

Substituting U_1 from (130) in (129) yields:

$$\forall k \neq 0 : U_2(k) = -(1 - \Gamma)\Gamma/2 \sum_{p+q=k} U_3(p) U_3(q), \quad (131)$$

which in turn can be substituted in (128):

$$\forall k : \quad \left(1 - \frac{\Gamma k^2}{\gamma^2} - (1 - \Gamma)U_2(0)\right) U_3(k) = -\frac{(1 - \Gamma)^2 \Gamma}{2} \sum_{p+q+r=k, p+q \neq 0} U_3(p) U_3(q) U_3(r). \quad (132)$$

Equation (132) can be used to predict the critical growth parameter. Indeed, before bifurcation, the ring is planar with $u_2 = \hat{u}_2/\gamma$, $u_1 = u_2 = 0$. Hence, $u_2^* = 1/\gamma = U_{2, \text{planar}}(0)$ and $\forall k \neq 0 : U_{2, \text{planar}}(k) = 0$. Furthermore, $U_{3, \text{planar}}(k) = 0$ and the bifurcation occurs when γ reaches a value such that a mode $U_3(k_0)$ does not vanish identically. Assuming that at the bifurcation, only one such mode exists, Equation (132) gives

$$\left(1 - \frac{\Gamma k_0^2}{\gamma^2} - \frac{(1 - \Gamma)}{\gamma}\right) U_3(k) = \left(-\frac{(1 - \Gamma)^2 \Gamma}{2} |U_3(k_0)|^2\right) U_3(k) \quad (133)$$

At the bifurcation, $|U_3(k_0)|^2 \ll 1$ and a bifurcation point is reached when the L.H.S. vanishes, that is

$$\gamma_{\text{crit.}} = \frac{1 - \Gamma + \sqrt{(1 - \Gamma)^2 + 4k_0^2 \Gamma}}{2}. \quad (134)$$

This result is consistent with the bifurcation analysis (71) and we conclude that the first transition occurs for $k_0 = 2$.

Beyond the bifurcation, there is a range of values of γ for which $|U_3(k)| \ll |U_3(k_0)| \forall k \neq k_0$. In that region, we propose a low dimensional model in terms of the key Fourier modes listed in Table 1. Note that although our choice was guided by a numerical study, (130) implies that $|U_1(k)| \ll |U_3(k_0)| \forall k \neq k_0$, and (131) yields $|U_2(k)| \ll |U_3(k_0)| \forall k \neq k_0$.

Truncating to the order given by Table 1, we obtain an approximation to (128):

$$U_1(k_0) = \frac{ik_0\Gamma}{\gamma} U_3(k_0), \quad (135)$$

$$\left(1 - \frac{k_0^2 \Gamma}{\gamma^2} - (1 - \Gamma)U_2(0)\right) U_3(k_0) = (1 - \Gamma)U_2(2k_0)U_3^\dagger(k_0), \quad (136)$$

$$\frac{2}{\gamma} U_2(2k_0) = -(1 - \Gamma)\Gamma U_3(k_0)^2. \quad (137)$$

Separating the complex Fourier modes U in module and complex phase, we obtain

$$U_1(k_0) = \rho_1 e^{i\varphi_1}, \quad U_2(0) = \rho_2 e^{i\varphi_2}, \quad U_3(k_0) = \rho_3 e^{i\varphi_3}, \quad \text{and} \quad U_2(2k_0) = \rho_4 e^{i\varphi_4}, \quad (138)$$

with $\rho_n \in \mathbb{R}^+$ and $\varphi_n \in [0, 2\pi]$, the underdetermined system (135) together with $U_n(k) = U_n^\dagger(k)$ gives:

$$\begin{aligned} \rho_1 &= \frac{k_0 \Gamma}{\gamma} \rho_3, & \varphi_1 &= \varphi_3 + \frac{\pi}{2}, \\ \rho_2 &= \frac{1 - \frac{k_0^2 \Gamma}{\gamma^2}}{1 - \Gamma} + \Gamma \frac{1 - \Gamma}{2} \rho_3^2, & \varphi_2 &= 0, \\ \rho_4 &= \Gamma \frac{1 - \Gamma}{2} \rho_3^2, & \varphi_4 &= 2\varphi_3 + \pi (= 2\varphi_1). \end{aligned} \quad (139)$$

If we define $\epsilon = \Gamma \frac{1 - \Gamma}{2} < 1/9 \ll 1$, then all other modes in (128-130) can be show to be $O(\epsilon^2)$.

$\mathbf{U}_n(k) = \frac{1}{2\pi} \int_0^{2\pi} \mathbf{u}_n(S^*) e^{-ikS^*} dS^*$		$\mathbf{D}_n(k) = \frac{1}{2\pi} \int_0^{2\pi} \mathbf{d}_n(S^*) e^{-ikS^*} dS^*$			
U_n	Non-vanishing modes	$\mathbf{D}_n \cdot \mathbf{d}_m$	Non-vanishing modes	$\mathbf{D}_n \cdot \mathbf{d}_a$	Non-vanishing modes
U_1	2	D_1^m	2	D_1^a	1,3
U_2	0,4	D_2^m	0,4	D_2^a	1,3,5
U_3	2	D_3^m	2	D_3^a	1,3

Table 1: List of dominant Fourier modes as found by the numerical simulation. The left column contains Fourier transform of \mathbf{u} components while the right columns list Fourier transform of components of the directors $\{\mathbf{d}_1, \mathbf{d}_2, \mathbf{d}_3\}$ along the angular momentum $\mathbf{d}_m = \mathbf{m}/|\mathbf{m}|$, and along an arbitrary direction \mathbf{d}_a perpendicular to \mathbf{d}_m .

The solution (139) of (125) still contains two unknowns: φ_3 and ρ_3 . The former is a free phase that can be arbitrarily chosen by setting a particular point on the ring as $S^* = 0$. On the other hand, we still need to find a condition for ρ_3 .

Expressing $\mathbf{d}_n(S^*)$ in Fourier series in (8) yields

$$\begin{aligned} \frac{ik}{\gamma} \mathbf{D}_1(k) &= \sum_{p+q=k} U_3(p) \mathbf{D}_2(q) - U_2(p) \mathbf{D}_3(q), \\ \frac{ik}{\gamma} \mathbf{D}_2(k) &= \sum_{p+q=k} U_1(p) \mathbf{D}_3(q) - U_3(p) \mathbf{D}_1(q), \\ \frac{ik}{\gamma} \mathbf{D}_3(k) &= \sum_{p+q=k} U_2(p) \mathbf{D}_1(q) - U_1(p) \mathbf{D}_2(q), \end{aligned} \quad (140)$$

where $\mathbf{D}_n(k) = \frac{1}{2\pi} \int_0^{2\pi} \mathbf{d}_n(S^*) e^{-ikS^*} dS^*$.

As $\frac{d\mathbf{m}}{dS} = 0$, the unit vector $\mathbf{d}_m = \mathbf{m}/|\mathbf{m}|$ is fixed in the lab frame. Let us define another fixed vector \mathbf{d}_a orthogonal to \mathbf{d}_m . When projected respectively on \mathbf{d}_a and \mathbf{d}_m , the system (140) is linear in the components of \mathbf{D}_s . Since each of the $\mathbf{D}_n(k)$ are Fourier modes of unit vectors, there must be a solution other than the trivial one and the determinant of the linear system must vanish. This gives the condition that fixes ρ_3 .

Indeed, projecting (140) on \mathbf{d}_a , and taking into account that only the modes listed in Table. 1 are active

gives

$$\frac{i}{\gamma} D_1^a(1) = U_3(2) D_2^{a\dagger}(1) + U_3^\dagger(2) D_2^a(3) - U_2(0) D_3^a(1) - U_2(4) D_3^{a\dagger}(3), \quad (141)$$

$$\frac{3i}{\gamma} D_1^a(3) = U_3(2) D_2^a(1) + U_3^\dagger(2) D_2^a(5) - U_2(0) D_3^a(3) - U_2(4) D_3^{a\dagger}(1), \quad (142)$$

$$\frac{i}{\gamma} D_2^a(1) = U_1(2) D_3^{a\dagger}(1) + U_1^\dagger(2) D_3^a(3) - U_3(2) D_1^{a\dagger}(1) - U_3^\dagger(2) D_1^a(3), \quad (143)$$

$$\frac{3i}{\gamma} D_2^a(3) = U_1(2) D_3^a(1) - U_3(2) D_1^a(1), \quad (144)$$

$$\frac{5i}{\gamma} D_2^a(5) = U_1(2) D_3^a(3) - U_3(2) D_1^a(3), \quad (145)$$

$$\frac{i}{\gamma} D_3^a(1) = U_2(0) D_1^a(1) + U_2(4) D_1^{a\dagger}(3) - U_1(2) D_2^{a\dagger}(1) - U_1^\dagger(2) D_2^a(3), \quad (146)$$

$$\frac{3i}{\gamma} D_3^a(3) = U_2(0) D_1^a(3) + U_2(4) D_1^{a\dagger}(1) - U_1(2) D_2^a(1) - U_1^\dagger(2) D_2^a(5), \quad (147)$$

where $D_n^a(k) := \mathbf{D}_n(k) \cdot \mathbf{d}_a$.

Substituting $D_2^a(k)$ s from (143,144,145) in (141-142) and (146-147) yields a 4×4 complex linear system in the D_1 s and D_3 s. This smaller system can be further simplified by the following change of complex variables that takes advantage of the definitions (138) and solutions (139)

$$x = D_1^a(1), \quad y = e^{i2\varphi_3} D_1^{a\dagger}(3), \quad z = \frac{i}{\gamma} D_3^a(1), \quad \text{and} \quad t = \frac{i}{\gamma} e^{i2\varphi_3} D_3^{a\dagger}(3), \quad (148)$$

so that

$$(141) \times \frac{i}{\gamma} \Leftrightarrow -\frac{x}{\gamma^2} + B(\gamma)z + \Gamma \frac{1-\Gamma}{2} \rho_3^2(z-t) = \frac{i}{\gamma} \left[U_3(2) D_2^{a\dagger}(1) + U_3^\dagger(2) D_2^a(3) \right], \quad (149)$$

$$(142)^\dagger \times \frac{ie^{i2\varphi_3}}{\gamma} \Leftrightarrow \frac{3y}{\gamma^2} + B(\gamma)t + \Gamma \frac{1-\Gamma}{2} \rho_3^2(t-z) = \frac{i}{\gamma} \left[U_3(2) D_2^{a\dagger}(1) + U_3(2) e^{i2\varphi_3} D_2^{a\dagger}(5) \right], \quad (150)$$

$$(146) \Leftrightarrow -B(\gamma)x + z + \Gamma \frac{1-\Gamma}{2} \rho_3^2(y-x) = \frac{2\Gamma i}{\gamma} \left[-U_3(2) D_2^{a\dagger}(1) + U_3^\dagger(2) D_2^a(3) \right], \quad (151)$$

$$(147)^\dagger \times e^{i2\varphi_3} \Leftrightarrow -B(\gamma)y - 3t + \Gamma \frac{1-\Gamma}{2} \rho_3^2(x-y) = \frac{2\Gamma i}{\gamma} \left[U_3(2) D_2^{a\dagger}(1) - U_3^\dagger(2) e^{i2\varphi_3} D_2^{a\dagger}(5) \right], \quad (152)$$

where $B(\gamma) = \left(1 - \frac{4\Gamma}{\gamma^2}\right) / (1 - \Gamma)$. Substituting (143-145) in (149-152) yields the system (linear in x, y, z , and t):

$$\begin{aligned} x \left(\frac{2\rho_3^2}{3} + \frac{1}{\gamma^2} \right) + y (\rho_3^2) + z \left(\left[\frac{8\Gamma}{3} - \epsilon \right] \rho_3^2 - B(\gamma) \right) + t (\rho_3^2 [-2\gamma + \epsilon]) &= 0, \\ x (\rho_3^2) + y \left(\frac{6\rho_3^2}{5} - \frac{3^2}{\gamma} \right) + z ([2\Gamma + \epsilon] \rho_3^2) + t \left(- \left[\frac{8\Gamma}{5} + \epsilon \right] \rho_3^2 - B(\gamma) \right) &= 0, \\ x \left(\left[-\frac{8\Gamma}{3} + \epsilon \right] \rho_3^2 + B(\gamma) \right) + y (-[2\Gamma + \epsilon] \rho_3^2) + z \left(-\frac{8\Gamma^2}{3} \rho_3^2 - 1 \right) + t (4\Gamma^2 \rho_3^2) &= 0, \\ x ([2\Gamma - \epsilon] \rho_3^2) + y \left(\left[\frac{8\Gamma}{5} + \epsilon \right] \rho_3^2 + B(\gamma) \right) + z (4\Gamma^2 \rho_3^2) + t \left(-\frac{24\Gamma^2}{5} \rho_3^2 + 3 \right) &= 0. \end{aligned} \quad (153)$$

Aside from the trivial solution $x = y = z = t = 0$, this linear system for x, y, z, t has a solution when its determinant vanishes. This condition yields a polynomial equation of degree 4 in ρ_3^2 , which when satisfied implies the existence of a non-trivial null-space vector and a non-planar solution for the ring. Figure 8 compares the amplitude of \mathbf{u}_3^* as found by numerical simulation to $2\rho_3$ obtained from the first positive root of this polynomial. It can be appreciated that this approximate solution cannot be distinguished from the numerical solution and covers the complete post-buckling shape of the ring up to the folding of the multi-covered ring and the next bifurcation point.